Chapter 2

MAGNETIC FIELD EVOLUTION

2.1 Magnetic Field in Neutron Stars

The observationally inferred strengths of the surface dipole magnetic fields of most of pulsars fall in the range $\sim 10^{12}$–10^{13} G as may be seen in Fig. 2.1. The origin of the field is thought to be due to flux freezing during the collapse of the core of the progenitor star: the magnetic flux in the core of the progenitor star is assumed to be conserved during the collapse resulting in field strengths as large as 10^{14}–10^{16} G in the neutron star. This was anticipated by Woltjer (1964) and Ginzburg (1964) before pulsars were discovered. The uncertainty in this hypothesis lies however in the lack of observational evidence for the field strengths in the core of massive stars. No measurements of the magnetic fields exist for mainsequence stars massive enough ($\gtrsim 8\ M_\odot$) to give birth to neutron stars. Among the somewhat lower mass stars, only the "chemically peculiar" have field strengths ~ 1000 G. The surface field in these cases is inferred to have a dipolar geometry with the dipole axis inclined at some random angle to the spin axis of the star. The structure of the interior field within the star is not known but there are evidences that a substantial part of the flux may reside in the core. The observed field in these lower mass stars in the upper mainsequence is thought to be generated by

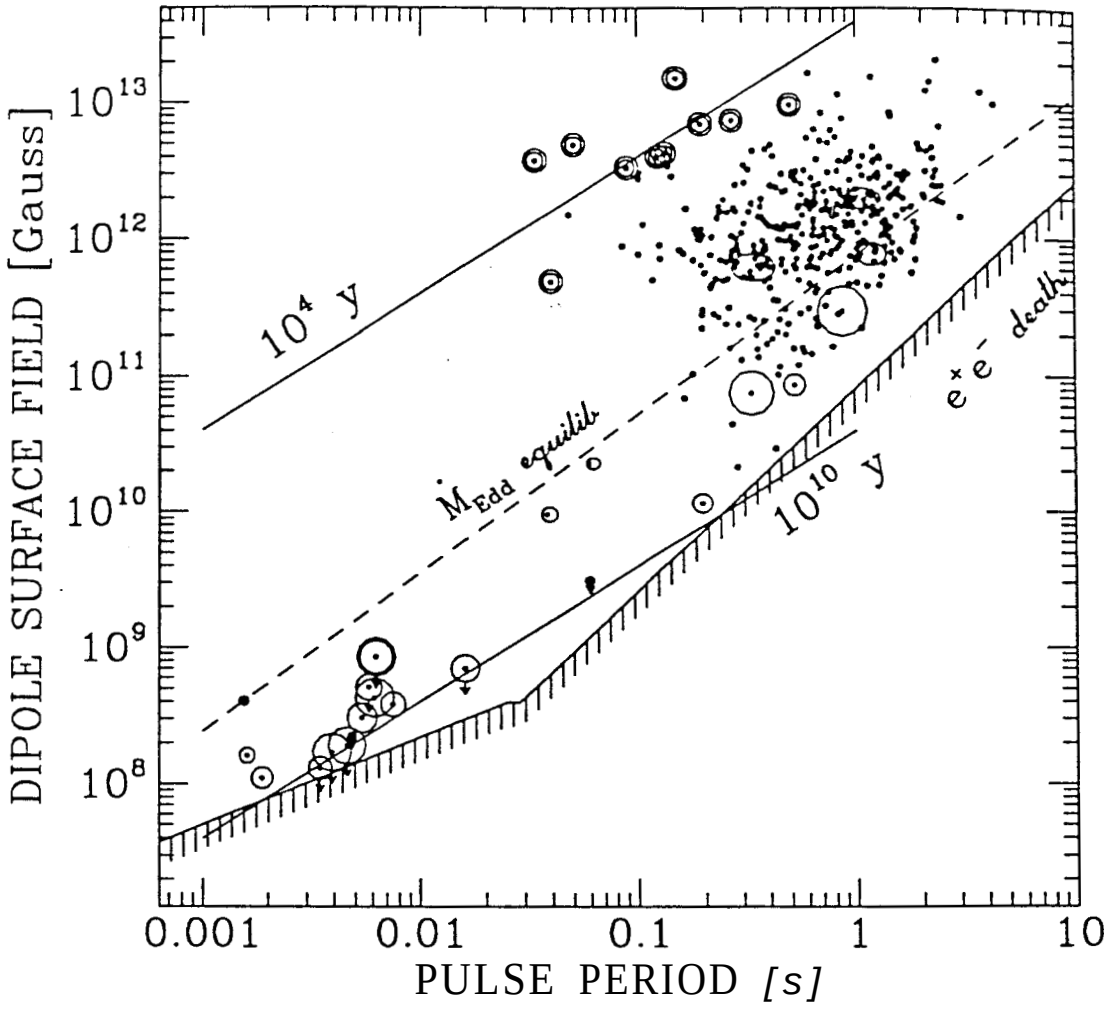

Figure 2.1- Distribution of the measured spin periods P_s and inferred surface dipole magnetic fields B_s of the observed Galactic and Magellanic Cloud radio pulsars. Single pulsars are shown by small *points.* Those surrounded by *double circles* are in supernova remnants. Binary pulsars are indicated by *ellipses* with the appropriate eccentricity of the orbit (which look like *circles* for the lower eccentricity systems). Two *solid* lines of the indicated constant characteristic ages, and the spin-up line corresponding to the Eddington accretion rate (the *dashed line)* are indicated. The *shaded boundary line* is the death-line discussed in § **2.3.** Note the absence of radio pulsars to the right of the death-line. The upper part of the death-line is that defined by the condition for pair generation in the magnetospheric gap (§ **2.3)** while the lower part is modified due to other effects mentioned in § **2.4.2.** Also note the near absence of disk-population radio pulsars in the region with field strengths in the range 10^9–10^{10} G which is referred to as the "gap" region. [adopted from Phinney & Kulkarni 1994]

dynamo processes occurring in their convective cores (Ruderman & Sutherland 1973; Borra, Landstreet & Mestel 1982). The same mechanism could be the source of the field in the cores of the more massive stars which finally collapse and form neutron stars. The frozen-in magnetic flux upon contraction will then result in an enhancement of the field in proportion to the squared of the ratio of the initial and final radii.

Alternatively, Blandford, Applegate & Hernquist (1983) have proposed that the magnetic field of a neutron star is generated after it is formed by *thermoelectric effects* in the crust. The outward flux of heat through the cooling crust of a newly born neutron star is shown to give rise to electric fields which could amplify an already existing seed magnetic field. The inward temperature gradient $\vec{\nabla}T_0$ drives an outward heat flux which is carried by the electrons. The existing seed field $\vec{B}_0$ will cause deflection of the otherwise radial trajectories of the electrons perpendicular to the field. The deflection of the (hotter and hence faster) outward moving electrons will be more than and in the opposite direction to the (colder and hence slower) inward moving electrons. A heat flux Q and an associated temperature gradient $\vec{\nabla}T_1$ would therefore develop in a direction perpendicular to both $\vec{\nabla}T_0$ and $\vec{B}_0$. The additional pressure gradient due to $\vec{\nabla}T_1$ has to be balanced by a thermoelectric field $\vec{E}_{\rm th}$. The field $\vec{E}_{\rm th}$ has a non-zero "curl" and thus a corresponding magnetic field $\vec{B}_1$ is generated in this process: $\vec{V} \times \vec{E}_{\rm th} = \frac{1}{c}\frac{\partial \vec{B}_1}{\partial t}$. The initial seed field $\vec{B}_0$ is hence amplified if the generated field $\vec{B}_1$ has a component parallel to it (viz. $\vec{B}_0.\vec{B}_1 > 0$) and if the growth rate is faster than the Ohmic dissipation rate. Furthermore the above mechanism is expected to be more efficient if a liquid layer is also present on the top of the solid crust which could enhance the seed field through dynamo processes as well (Blandford et al. 1983, Urpin, Levshakov & Yakovlev 1986).

In the latter mechanism for the field generation the magnetic flux is expected to be constrained within only the crusts of neutron stars. The scale length of the generated field by the thermoelectric effects is characterized by the size of the region with highest temperature gradient $\vec{\nabla}T_0$ which is of the order of the melting depth $\sim$ 100 m. The newly generated flux in this region would diffuse inward but it will mainly remain

confined to the outer layers of the crust which has a thickness $\gtrsim 1$ km. The highly conductive diamagnetic (or superconductive) core of a neutron star would not permit the newly generated field to penetrate into it. In contrast if the field is that amplified (or generated) during the collapse of the progenitor core then the flux is expected to permeate the whole neutron star more or less uniformly.

The magnetic field of a star of radius R and *uniform* conductivity a is expected to decay exponentially with a time scale

$$\frac{4\,\sigma\,R^2}{\pi\,c^2} \tag{2.1}$$

A crust limited field would likewise decay on the Ohmic time scale

$$\tau_{\rm Ohm} = \frac{4\,\pi\,\sigma_c\,L^2}{c^2} \tag{2.2}$$

where a, is the mean electrical conductivity in the crust, and L is the thickness of the crust which is assumed to the characteristic length scale for the currents (Cowling 1957, p. 5). A study of the evolution of the magnetic field in the crust of neutron stars has revealed that contrary to the above expectation it behaves differently than a purely exponential decay. The calculations predict an initial decay by only a factor e on the expected time scale of $\tau_{\rm Ohm} \sim 10^7$ yr for the given conductivity of the crust. The decay rate is however found to be slowed down at later times due to the inward diffusion of the flux toward the higher conductivity regions (Sang & Chanmugam 1987). The overall decay time scale of the magnetic field of neutron stars even if it is restricted to only the crust is therefore expected to be much larger than the value of $\tau_{\rm Ohm}$ given by Eq. 2.2.

On the other hand, the fossil field would be threading through the stellar core as well as the crust. The very large conductivity of the core of neutron stars would imply an Ohmic decay time scale $> 10^{12}$ yr for the core component of the field (Baym, Pethick & Pines 1969). Nevertheless, for a "normal" (ie. non-superconducting) *fluid* core in order to support a dipolar magnetic field the field is required to be stabilized by currents passing through the crust (Flowers & Ruderman 1977). The field in the fluid core would otherwise decay rapidly on the associated MHD relaxation time scale

which would be as short as few years. Different sub-volumes of the core would tend to rotate upside-down with respect to the magnetic axis such that opposite poles come close and cancel each other. The field stabilization might be achieved either by freezing of the flux in a crystalized crust and/or (even before that) by a strong toroidal field in the crust. The MHD relaxation mechanism cannot then proceed since it requires the toroidal field lines to be twisted and thus the field energy to be increased. In either case the lifetime of the supporting currents in the crust and hence the decay time scale of the dipole field in the normal fluid core of the star would be still decided by the Ohmic dissipation time scale $\tau_{\rm Ohm}$ of the crust.

The picture changes drastically when the superconductivity of the protons in the fluid core of the star is taken into account. A fundamentally important property of a superconductor is its dimagnetic behavior in expelling an applied magnetic field (the Meissner effect). This effect is however limited to fields smaller than a thermodynamic critical value $H_{\rm cr}$. For applied fields larger than $H_{\rm cr}$ superconductivity is destroyed. Nevertheless magnetic field might penetrate into a sample without destroying its overall superconducting state. The way this happens is different in the two different types of superconductors. A type-I (type-11) superconductor is the one for which the London penetration depth λ is smaller (larger) than BCS correlation length ξ $[\times\sqrt{2}]$. In the type-I at some values of the applied field $\lesssim H_{\rm cr}$ the whole body forms a finely divided laminar structure of alternate superconducting and normal domains with surfaces parallel to the field direction and thicknesses so that all the penetrating field is carried by the normal lamellae. The strength of the field at and above which this transition to the so-called intermediate state occurs depends on the shape of the sample; for a sphere it is $\frac{2}{3}H_{\rm cr}$. In type-I1 superconductors on the other hand the field penetration is achieved over a comparatively wide range of field values between two critical values $(H_{\rm c1} < H_{\rm cr} < H_{\rm c2})$ which are independent of the shape of the body.

The existing field in the interior of a neutron star at the time of its transition to proton-superconductivity is, however, much smailer than $H_{\rm c1}$. According to the usual laboratory experience this should imply a complete Meissner expulsion of the flux from

the core into the crust at the onset of core-superconductivity. However due to the very large conductivity of the matter in the interior of a neutron star it is argued that *the flux* might *not be expelled* during the transition of the core to a superconducting state (Baym, Pethick & Pines 1969). The resistivity in the "normal" phase is decided by scattering of electrons off the protons which are extremely degenerate and result in a very large value for the conductivity $\sim 1.5 \times 10^{29}\ s^{-1}$ (compare with that of copper being $\lesssim 10^{18}\ s^{-1}$). The associated Ohmic decay time scale for a neutron star of 10 km radius $\tau_{core} \sim \frac{4\sigma R_c^2}{\pi c^2} \sim 10^{13}$ yr, where R_c is the radius of the core. The expulsion time scale for the field present at the onset of superconductivity in the core is thus estimated to be $\sim \frac{B_c^2}{H_{crit}^2}\tau_{core} \sim 10^8$ yr, where B_c is the strength of the existing uniform field in the core of the star. This is simply because nucleation of the superconductivity and the expected initial expulsion of the flux out of a central part of the core due to the Meissner effect could only proceed until a maximum size of the flux-free superconducting central region is achieved. Namely the growth of the nucleation will be stopped when the cross sectional radius of the inner region (perpendicular to the magnetic field) reaches a maximum value R_M such that the swept out field into the normal outer region reaches the value of the critical field H_{crit}. Further growth of the inner superconducting region and expulsion of the field will make the field at its surface larger than H_{crit} which will either destroy the superconductivity of the interior region (type-I) or else cause the field to penetrate into it (type-11). If superconductivity of the core as a whole is to be in a flux free Meissner phase the relevant expulsion time scale would be therefore same as the decay time scale of the accumulated flux in the outer region (with a characteristic thickness $\sim R_c - R_M$). Thus, R_M could be determined from the condition

$$B_c\, \pi R_c^2 = H_{crit}^2\, 2\pi R_M (R_c - R_M) \tag{2.3}$$

where it is assumed that $(R_c - R_M) << R_c$ because $B_c << H_{crit}$. From Eq. 2.3 one obtains

$$\frac{R_c - R_M}{R_c} \sim \frac{B_c}{H_{crit}} \tag{2.4}$$

The decay time scale of the field in the outer region would be $\sim \left(\frac{R_c - R_M}{R_c}\right)^2 \tau_{core}$ (Eq. 2.1)

which together with Eq. 2.4 verify the above estimate for the expulsion time scale. Superconductivity of the protons in the interior of a neutron star therefore sets in without expelling the existing field B_i.

The protons in the core of a neutron star are believed to form a type II superconductor since for protons the penetration depth $\lambda_p \sim 10^{-11}$ cm and the coherence length $\xi_p \sim$ few $\times 10^{-13}$ cm. The penetrated flux in the mixed state (or Shubnikov phase) of a type-II superconductor is arranged in the form of a lattice of microscopic flux tubes (fluxoids) each carrying a quantum of flux

$$\begin{aligned} \phi_0 &= \frac{hc}{2e} \\ &= 2 \times 10^{-7} \text{ G cm}^2 \end{aligned} \tag{2.5}$$

The magnetic field in the fluid core is expected likewise to be bunched into the fluxoids forming a triangular uniform lattice (Abrikosov lattice) as in the mixed state (see Fig. 2.2).

The field of each fluxoid falls off exponentially with distance from the axis of the fluxoid for large distances ($>> \lambda_p$) while close to the axis it follows a logarithmic dependence. The average field inside a fluxoid is therefore estimated as $B_\phi \sim \frac{\phi_0}{\pi\lambda_p^2} \sim 2 \times 10^{15}$ G. The field configuration changes from its confined geometry within the fluxoids in the core of the star to an almost uniform field threading through the interstitial spaces between nuclei in the crust. The turn over in the field geometry occurs over a short length scale ($\sim \lambda_p$) above the transition surface between the solid crust of nuclei to the fluid core quantum liquid. The stability of the field geometry against the large gradient of the magnetic pressure across the turn over region is achieved by a balancing force due to deformation of the transition surface from local planarity. The force arises because of the surface tension associated with the first-order transition of the nuclei to the core liquid (Harvey et. al. 1986).

The magnetic flux frozen into the core superconductor is of course expected to survive *indefinitely except if fluxoids are driven out* of the superconductor by some "external" agent. Our studies of the field decay in neutron stars in this and the following chapter adopt this viewpoint. In the present chapter predictions of the original model of

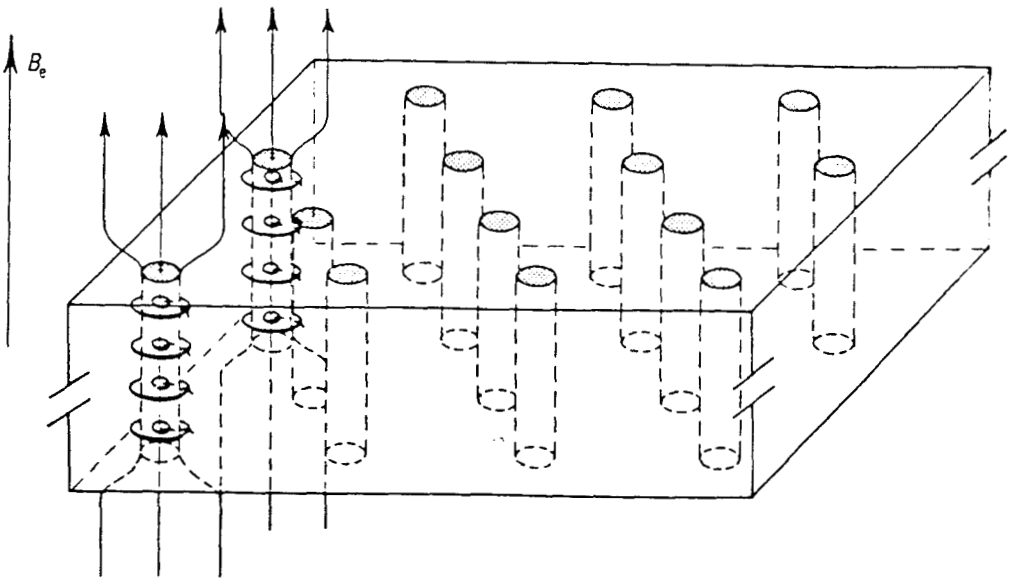

Figure 2.2**(a)-** Schematic representation of the Abrikosov fluxoids in the mixed state (the Shubnikov phase) of a type-I1 superconductor. Magnetic field and suppercurrent are only illustrated for two flux tubes. [from Buckel 1991]

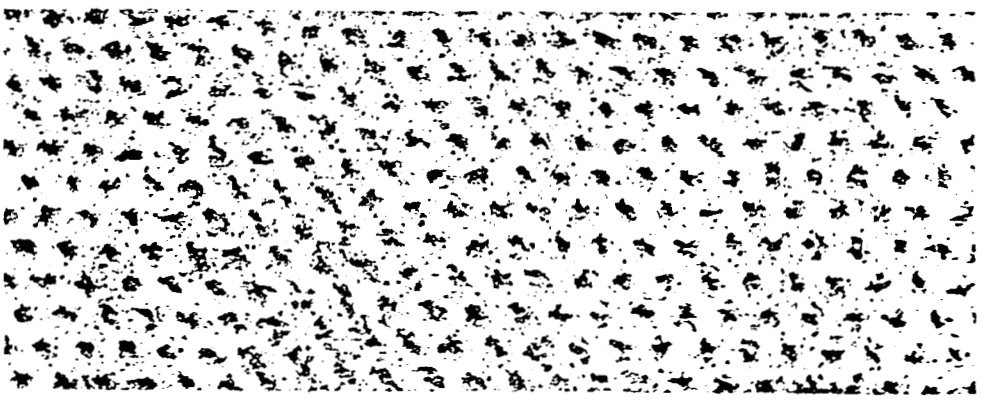

Figure 2.2(b)- Direct observation of the ***individual*** flux lines (the Abrikosov fluxoids) in the mixed state of a type-I1 superconductor. The fluxoids are arranged in a regular triangular lattice (Mag. 9000×). Colloidal particles with diameters of less than 50 nm formed from evaporated iron are made to sediment slowly onto the surface of the superconductor out of which flux tubes are emerging. Each tube contains one flux quantum ϕ_0 as indicated in Fig. 2.2a for two flux tubes. The ferromagnetic colloidal iron particles deposit at those places where the flux tubes emerge from the surface since the strongest fields are to be found there. It is thus possible to decorate the flux tubes' spouts and then use the methods of electron microscopy to make the structure visible. The picture is due to Essman & Trauble 1967. [from Buckel 1991]

spin-down-induced flux expulsion (Srinivasan et al. 1990) are explored. The "external" agent which drives the fluxoids out of the core in this model is the pinning of the fluxoids with the neutron vortices. In chapter 3 the picture is expanded by bringing in the role of the other forces acting on the fluxoids in the core of a neutron star, in addition to the pinning force.

The decay of the surface field of neutron stars in these models is nevertheless still governed by the Ohmic time scale for the expelled flux within the crust. However it has to be noted that the inward diffusion of the flux in the crust which was found (Sang & Chanmugam 1987) to cause an increase in the effective decay scale of the crust is not expected to occur in these models. The Ohmic decay time scale of the crust in this case is just that due to the exponential decay in the crust associated with the conductivity of the crustal matter (Bhattacharya & Datta 1996).

2.1.1 The Fields of X-ray Pulsars versus Recycled Radio Pulsars

Neutron stars are generally detected as either rotation-powered radio pulsars (being single or in a binary normally with another compact stellar remnant) or accretion-powered X-ray sources in binary systems. Rotation periods and surface magnetic fields assigned to the neutron stars in these two different types of systems and even in their observationally distinct subclasses are found nonetheless to span different ranges of values.

The low magnetic field strengths of binary pulsars, millisecond pulsars, and pulsars in globular clusters, all believed to be old neutron stars, strongly support the idea of magnetic field decay in neutron stars. On the other hand, the present field strengths ($\gtrsim 10^8$ G) of these objects seem to be stable (van den Heuvel, van Paradijs & Taam 1986; Kulkarni 1986; Bhattacharya & Srinivasan 1986) thus ruling out a simple spontaneous Ohmic decay as the cause of the earlier field reduction in these objects. An exponential decay with a time constant even of the order of 10^8 yr would result in negligibly small values for the strengths of the magnetic field in neutron stars with ages more than few

$\times 10^9$ yr. Most of the above mentioned short-spin period low-magnetic field pulsars are indeed believed to be old neutron stars "recycled" (ie. spun-up during a Roche-lobe overflow mass transfer) in Low-Mass X-ray Binaries (LMXBs) (Radhakrishnan & Srinivasan 1984; Alpar et al. 1982).

The observed differences in the spin periods has been explained through the effects of the interaction of magnetosphere of a neutron star with the matter accreted from its mass-losing companion in a binary system (eg. Pringle & Rees 1972; Illarionov & Sunyaev 1975). Certain evolutionary routes among various systems have been hence established with additional constraints on the expected ages and lifetimes of neutron stars in the various systems(eg. Taam & van den Heuvel 1986). The evolution of the magnetic field has to therefore not only account for the observed range of the field strengths in the different types of sources it should be also consistent with the requirements of the spin evolution of neutron stars in binaries. The popular belief is that young pulsars possess strong magnetic fields $\gtrsim 10^{12}$ G which might at least under some conditions that is apparently connected with a binary history of the star, decay down to values $\sim 10^8$ G. While the issue of the field decay in isolated radio pulsars has remained controversial since their discovery the association between the presence of neutron stars in close binaries and their field decay has been generally accepted following the discovery of low-field binary and millisecond pulsars (see eg. the review by Srinivasan 1989).

The strength of the surface dipole magnetic field of radio pulsars is usually estimated by assuming that the observed spin-down of the star is due to a torque same as that of a magnetic dipole of the same strength rotating perpendicular to its axis in vacuum :

$$I\,\dot{\Omega} \;=\; -\frac{2}{3c^3}\,B_s^2\,R_s^6\,\Omega^3 \tag{2.6}$$

From this one obtains

$$\begin{aligned} B_s \;&=\; \left(\frac{3c^3\,I\,P_s\,\dot{P}_s}{8\pi^2\,R_s^6}\right)^{\frac{1}{2}} \\ &=\; 3.2\times 10^{19}\,\left(P_s\,\dot{P}_s\right)^{\frac{1}{2}}\;\;\mathrm{G} \end{aligned} \tag{2.7}$$

where P_s and $\dot{P}_s$ are in units of seconds and s s^{-1}, respectively. It is important to note

however that observationally there exists no direct and model independent measurement of the strengths of the dipole magnetic fields of neutron stars. Also, theoretically there is no consensus regarding the origin as well as the structure and distribution of the fields inside these stars.

The inferred field strengths of the observed binary pulsars in double neutron star systems (such as PSR 1913+16) are on the other hand ~ 2 orders of magnitudes smaller than that usually assumed for HMXBs which are presumably their immediate progenitors. The normal Ohmic decay of the field in the crust for any given value of $\tau_{Ohm} \gtrsim 10^6$ yr cannot be clearly the effective mechanism for such a reduction in the surface fields since the assumed transition from the X-ray phase to the birth of the recycled pulsar is expected to occur over a period $\lesssim 10^6$ yr. A short-term enhanced field decay (see § 2.4.3) occurring at the final stages of the X-ray phase in HMXBs has to be invoked in order to account for the apparently large differences in magnetic fields of the neutron stars at these successive phases of their binary evolution. Alternatively, one might argue that the observed double neutron star systems have descended from a possibly low-field sub-class of HMXBs which might not also show any regular pulsation in their observed X-ray emissions. In fact, field strengths as low as $\sim 10^9$ G has been suggested even for some of the pulsating HMXB sources (Ruderman 1987). Hence, while the low-field HMXBs could be considered as the progenitors of recycled pulsars similar to PSR 1913+16, the strong-field pulsating HMXBs would be expected to result in recycled pulsars which will first show up in the "injection" region (cf. § 2.3.1). The latter objects will evolve rapidly along vertical tracks which extend in most cases down below the "death"-line shown in Fig. 2.1, as will be discussed in § 2.3 and § 2.4.3.

The apparent inconsistency in the strengths of the magnetic fields in the above two classes of objects should be however treated cautiously since the existing estimates of the *dipolar* fields of neutron stars in HMXBs are subject to large uncertainties. The direct observational measurements based on the frequencies of the observed cyclotron X-ray absorption lines in some of these sources reflect in principle only the ***local*** field strengths in the X-ray emission region which need not be the same as the dipolar field

of the star (Flowers & Ruderman 1977; Srinivasan & van den Heuvel 1982). The spin behavior of an accreting neutron star is on the other hand used to estimate its *dipolar* field based on the predictions of the accretion torque theory (Ghosh & Lamb 1979). Uncertainties in the theory and also in simultaneously measuring the spin-up or spin-down rates and the accretion luminosities (as is required in the theory) lead however to large uncertainties in the inferred values for the magnetic fields.

2.2 Spin-down-Induced Flux-expulsion (SIF)

A model for the evolution of the magnetic field in neutron stars has been proposed which relates it to the spin evolution of the star in an essential way (Srinivasan 1989; Srinivasan et al. 1990). An increase in the spin period of a neutron star has been suggested to result in a decrease in the strength of the stellar magnetic field which is assumed to be embedded in the superfluid-superconductor interior of the star. The magnetic flux is assumed to be transported out of the core, at the same rate as of the spin-down of the star, into the crust where it is expected to decay subsequently. The evolution of the external surface field of a pulsar is hence determined in this scenario by its spin-down history and the decay time scale of the magnetic flux in the crust.

2.2.1 The Mechanism

In the Spin-down-Induced Flux expulsion (SIF) model, *the pinning between the neutron vortices and the proton fluxoids in the superfluid core of a neutron star causes the magnetic flux to be expelled into the core-crust boundary as the star spins down.* The core of a neutron star is believed to consist mainly of neutrons in a superfluid state and protons in a superconductor state, the latter contributing only to a small fraction of the total mass. The rotating core superfluid is furthermore expected to be in a vortex state with approximately $2 \times 10^{16} P_s^{-1}$ vortices parallel to the rotation axis of the star, where P_s is the spin period in units of seconds. Since the superfluid state may be represented by a single macroscopic wave function $\Psi(\vec{R}) = |\Psi| e^{i\Theta(\vec{R})}$ throughout the

condensate, the superfluid velocity field $\vec{v_s} \propto \vec{\nabla}\Theta$ which shows that a bulk superfluid rotation (which requires $\vec{\nabla} \times \vec{v_s} \neq 0$) is impossible except around existing singularity points of the wave function. A superfluid is therefore expected to mimic a nearly rigid-body rotation (as normal fluids) by formation of quantized vortices within which the density of the superfluid matter approaches zero. The presence of the vortices and the dependence of their number and distribution on the rotation rate in a rotating sample of superfluid Helium has been verified in laboratory experiments (see Fig. **2.3).** These are the entities which carry the angular momentum associated with the bulk rotation of a superfluid (in the case of neutron superfluid in the core of a neutron star) and their total number has to decrease through their outward motion in order for the superfluid to spin down.

An assumed frozen-in magnetic flux in the core of a neutron star is also believed to be confined within the cores of $\sim 10^{19} B_c$ fluxoids which are parallel to the magnetic axis of the star, where B_c is the average field strength in the core in units of Gauss. A reduction in the number of these flux lines corresponds to a reduction in the magnetic field strength in the core of a neutron star. The proton fluxoids and the neutron vortex lines are furthermore expected to act as pinning sites for one another. The pinning is associated with an energy barrier for or against an overlap of the two vortex-structures which are both magnetized and consist of normal non-superfluid matter close to their axes (Muslimov & Tsygan 1985; Sauls 1989). The resulting effective pinning force is estimated to be $\sim (0.1 - 1.0) \times 10^6$ dyne per connection for the different suggested interaction mechanisms (Sauls 1989; Srinivasan et al. 1990; Bhattacharya & Srinivasan 1991). The radially outward motion of the neutron vortices due to the spin-down of the star is therefore suggested to induce a field decay in the core assuming that the fluxoids are also swept out along with the vortices due to their interpinning (see Fig. **2.4).** In the original model of SIF of Srinivasan et al. (1990) it was suggested that the rate of this sweeping is complete namely the fractional change in the number of fluxoids is same as that of the vortices. In *other words the two types of the lines were assumed to move with the same radial velocity at all times.*

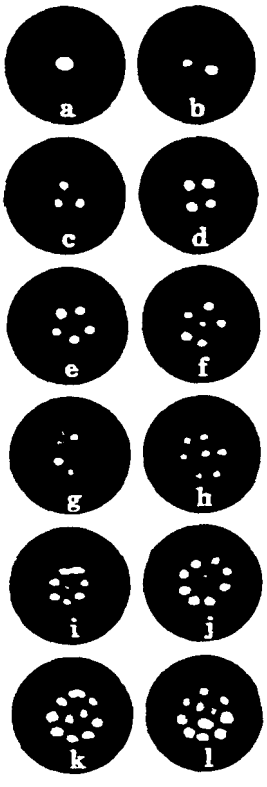

Figure 2.3- Photograph of stable vortex arrays in rotating superfluid Helium. Different pictures (dark circles) show states with vortex numbers from 1 to 11, and correspond to angular frequencies between 0.30 s^{-1} to 0.86 s^{-1}. However the correspondence between the observed vortex number in the successive pictures and the rotation rate is not monotonic. The particular state of the superfluid is not determined by the current rotation rate alone but also by its *past history* as well. Monotonic acceleration from rest produces a state with fewer vortices than predicted for the given rotation rate, apparently due to the effect of pinning of the vortices to the walls of the bucket. The diameter of the dark circles correspond to the 2 mm bucket diameter. The actual location of the bucket relative to the arrays is not known and the arrays were manually superimposed symmetrically within the circles. The basic technique to record the vortex line's position utilizes electron bubbles (ions) trapped in the core of a vortex. This trapped charge is extracted through the fluid's meniscus (where the vortex meets the free surface) and is then imaged onto a phosphor screen, amplified, and recorded. [from Yaemchuk & Gordon 1979]

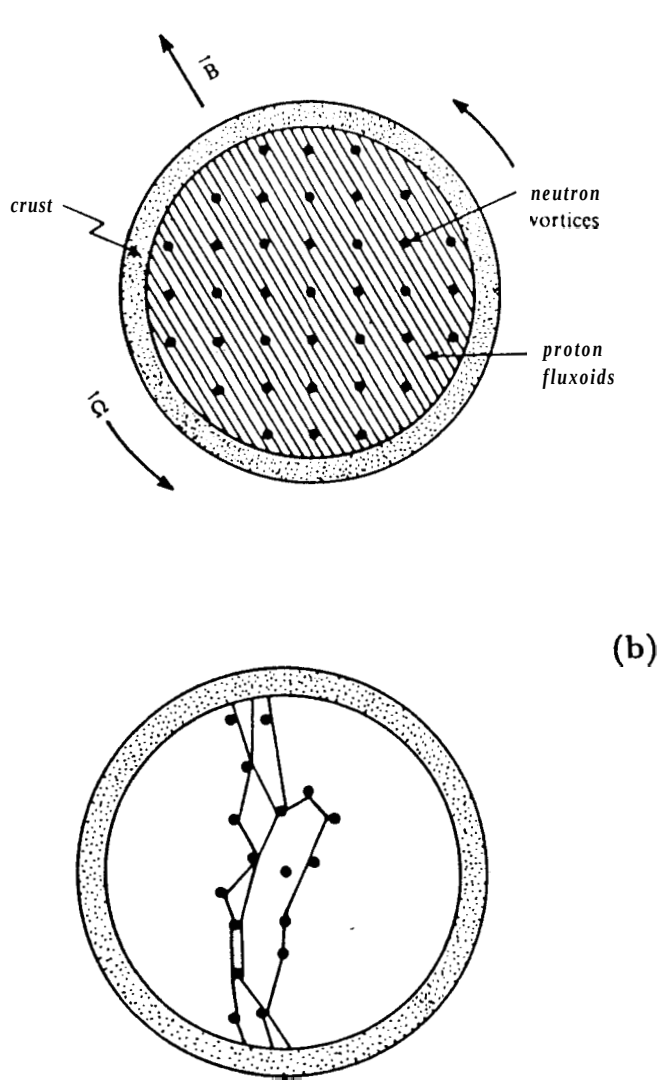

Figure 2.4- a) A view of the equatorial plane of the core of a rotating neutron star showing an idealized geometry of the arrangement of the neutron superfluid vortices (parallel to the rotation axis) and the proton superconductor fluxoids (parallel to the magnetic axis). For the purpose of illustration the magnetic axis has been assumed to be perpendicular to the rotation axis. b) A more realistic state of affairs in the presence of strong interaction between the vortices in the two superfluid mixture. [from Srinivasan et al. 19901

A more detailed treatment of the dynamics of fluxoids motion should however take into account all the other forces which might act on them and should also allow for the finite strength of the pinning force and hence for the possibility of the two types of lines moving with different velocities and overtaking each other. The effects of such considerations on the magnetic evolution of neutron stars have already been investigated by Ding, Cheng & Chau (1993), although they restricted themselves to the case of a dipole spin-down phase which is applicable only to solitary pulsars. In this chapter we will follow the prescription of the original SIF model by *assuming that the rate of the expulsion of the magnetic flux out of the core is always equal to the spin-down rate of the star*. Thus the following expression will be used for calculating the rate of the flux expulsion out of the core of neutron stars for given spin-down rates:

$$\frac{\dot{B}_c}{B_c} = -\frac{\dot{P}_s}{P_s} \tag{2.8}$$

where a dot denotes a time derivative of the respective quantity. The coupled dynamics of the fluxoids and the vortices will be discussed in the next chapter.

Given a superfluid-superconductor mixture in the interior of a rotating magnetized neutron star together with the associated neutron and proton vortices the distribution and the geometry of these vortex lines is further uncertain. Neutron vortices are thought to form a uniform triangular lattice of straight lines parallel to the spin axis (Ruderman & Sutherland 1974) which could however be subject to a radial gradient of the number density of the lines supporting differential rotation of the neutron superfluid. The fluxoids could have a distorted and entangled geometry as it is found to occur in laboratory superconductors (Nelson 1988; Huse, Fisher & Fisher). A stabilizing toroidal field component might be also present in the fluid core of a neutron star in addition to the dipolar field, should the crystalization of the crust does not take place early enough (Flowers & Ruderman 1977). The toroidal component present at the onset of superconductivity in the core would result in a complicated distorted geometry of the fluxoids. Such geometries of lines would indeed further increase the effectiveness of their suggested inter-pinning with the vortices even though two inclined uniform lattices of parallel lines would be sufficient to do the job, viz. take the fluxoids

out along with the vortices.

The predicted behavior of the surface field of neutron stars according to the SIF model depends on the rate of decay of the expelled magnetic flux within the crust. The Ohmic decay of the currents in the crust is however subject to uncertainties about the correct value of the conductivity of the matter in the crust. Also, the assumed distribution and boundary conditions of the magnetic flux in the crust further affects the inferred effective rate of its decay as mentioned earlier (§ 2.1). The evolution of the field in the crust is further complicated due to other possible processes namely a radial Hall drift of the expelled flux and an associated turbulent cascade mechanism for the currents in the crust which could result in a redistribution of the field and hence a change in the rate of its final Ohmic decay (Jones 1988; Goldreich & Reisenegger 1992). Different values for the effective decay time scale of the field in the crust are therefore used in our model computations in order to explore various possibilities.

2.2.2 General Predictions of the SIF Model

The coupled evolution of spin periods and magnetic fields as predicted in this model has different bearings for the single neutron stars which are subject only to the persistent decelerating dipole torque, in contrast to those in close binaries. In the latter case interaction of the magnetosphere with the matter accreted from the stellar wind of a companion star may result in torques of either signs and varying magnitudes which act on the neutron star at the various stages of its evolution. This model predicts that while the fields of the isolated neutron stars which have only a small rate of slowing down may not decay significantly, those of the first-born neutron stars in binaries would decay substantially because of the spin-down to very long periods that can occur in these systems. As had been already pointed out (see Fig. 2.5) the maximum spin period P_{max} to which the neutron star is slowed down during the "propeller" phase will uniquely determine the final value of the residual magnetic field in the recycled pulsar that will be born at the end of the accretion phase of the binary (Srinivasan et al. 1990).

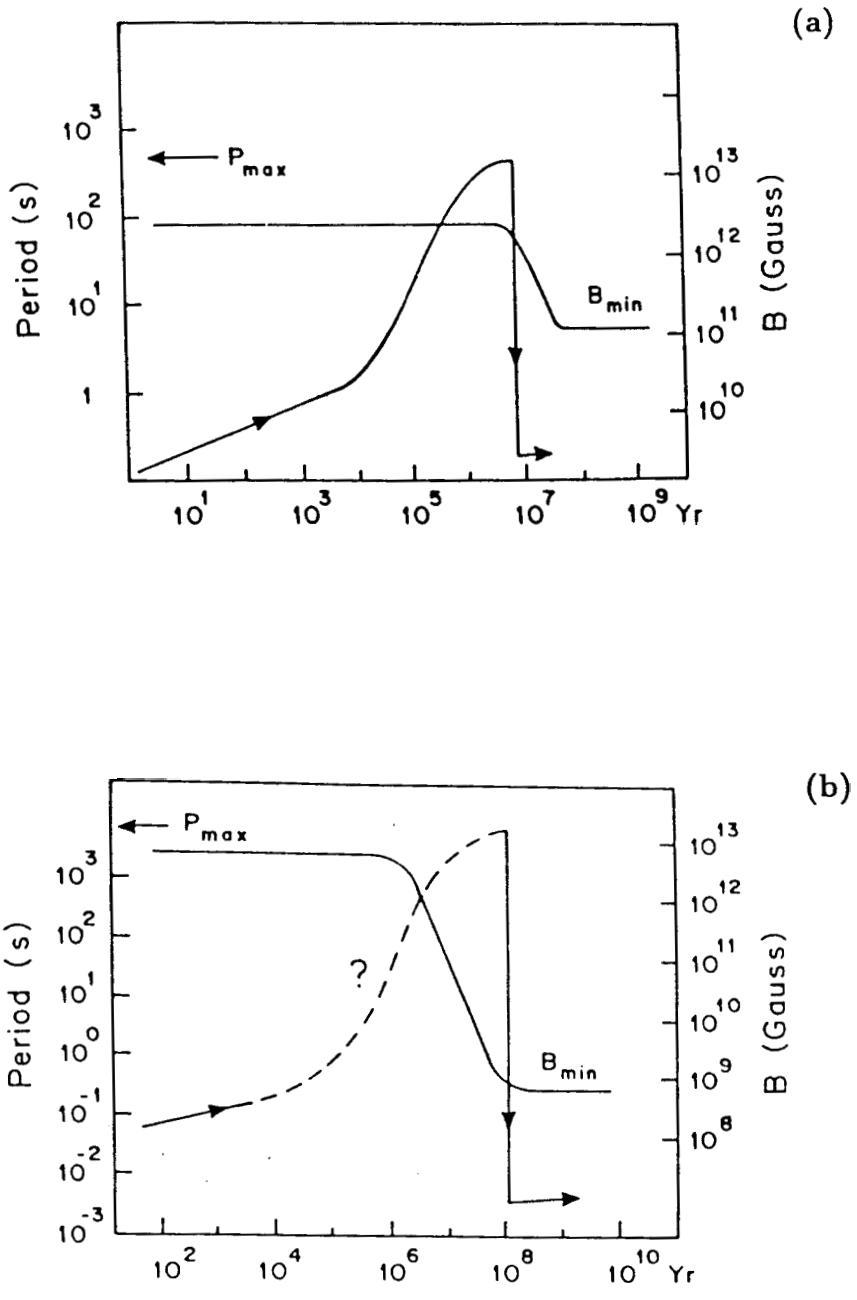

Figure 2.5- The rotational history and the evolution of the magnetic field of neutron stars in binaries. Figure a is appropriate for the case of neutron stars in a binary with a massive companion whose mainsequence lifetime $t_c \lesssim \tau_{Ohm}$ the field decay time scale in the crust. In this case the decay of the field will lag behind the rapid period lengthening. The asymptotic field will be determined by the maximum period to which the neutron star is slowed down. Figure b is for the case when $t_c >> \tau_{Ohm}$ which may obtain in low-mass binaries. Here the field decay will 'track' the period of rotation. [from Srinivasan et al. 19901

The quantity P_{max} plays a special role in determining the properties and final fates of the recycled pulsars. The strength of the surface magnetic field B_R of a pulsar just after recycling as predicted in SIF is given (approximating the time interval between achieving P_{max} and P_{eq} in the binary to be comparable with the mainsequence lifetime of the companion star t_c; see Fig. *1.2* for this and a recapitulation of the meaning of the various quantities used in the present discussion) as:

$$\begin{aligned} B_R &\approx (B_i - B_f)\, e^{-\frac{t_c}{\tau_{Ohm}}} + B_f \\ &\approx B_i\, e^{-\frac{t_c}{\tau_{Ohm}}} + B_f \end{aligned} \tag{2.9}$$

where τ_{Ohm} is the decay time scale of the magnetic field in the crust, and B_f is the predicted final value of the field given as:

$$B_f = \left(\frac{P_{max}}{P_i}\right)^{-1} B_i \tag{2.10}$$

The post-recycling evolution of the pulsar will further depend on the ratio $\frac{t_{sd}}{\tau_{Ohm}}$, where t_{sd} is the characteristic spin-down age of a pulsar and is defined as

$$\begin{aligned} t_{sd} &= \frac{P_s}{2\dot{P}_s} \\ &= 1.6 \times 10^7 \left(\frac{P_s}{B_{12}}\right)^2 \text{ yr} \end{aligned} \tag{2.11}$$

where $B_{12}^2 = 10^{15} P_s \dot{P}_s$ has been assumed, B_{12} is the surface field strength B_s in units of 10^{12} G, and P_s is in units of seconds. Assuming a ratio of $\frac{B_i}{B_f} = \frac{P_{max}}{P_i} \sim 2 \times 10^4$ (which is suggested by our model computations discussed in **§ 2.4)** to prevail for most of the recycled pulsars two distinct classes of recycled pulsars are thus distinguished, based on the corresponding values of $\frac{t_c}{\tau_{Ohm}}$:

1. In systems with a $\frac{t_c}{\tau_{Ohm}} \gtrsim 10$ (ie. $e^{\frac{t_c}{\tau_{Ohm}}} \sim \frac{P_{max}}{P_i} \sim 2 \times 10^4$) *the flux expelled out of the core of the neutron star into its crust would have completely decayed by the time the recycled pulsar starts its new life, and no further field decay is expected during the subsequent evolution of the recycled pulsar,* namely $B_f \sim B_R$.

2. Binaries with a $\frac{t_c}{\tau_{Ohm}} < 10$, on the other hand, would be subject to further magnetic decay while functioning as a recycled pulsar. Two subclasses are,

in principle, possible among these pulsars which are expected to experience a so-called "delayed" field decay (Srinivasan et al. 1990):

a) If $t_{sd} < \tau_{Ohm}$ at and around the P_{eq} from which the recycled pulsar starts off, it will initially move along a constant magnetic field path on the $B_s - P_s$ plane. Such pulsars will eventually acquire long enough periods corresponding to values of $t_{sd} > \tau_{Ohm}$ and their evolutionary tracks would therefore bend down and cross the death line vertically.

b) In the other extreme where the condition $t_{sd} >> \tau_{Ohm}$ is satisfied at the given P_{eq}, the evolution of the pulsar would be along a vertical path and at a constant period (equal to its P_{eq}) until its field decays to the final expected residual value. The pulsar would then evolve along a constant field track, if its downward evolution had not already crossed the death-line.

From the above discussion it is clear that the behavior of pulsars recycled in low-mass long-lived systems is determined basically by the values of P_{max} which they have attained at some stages in their past histories. On the other hand, the dominant factor in the case of those descended from short-lived massive binaries is the Ohmic time scale τ_{Ohm}. The predicted behavior of the latter systems is therefore expected to be more sensitive to and hence might be used along with the corresponding observational data to further constrain the assumed value of τ_{Ohm}.

In this chapter we explore this problem quantitatively, and ask under what conditions would such an evolution best reproduce the observed properties of young as well as old neutron stars. We consider a simple model for the evolution of neutron stars in binary systems as well as single pulsars, taking into account the spin-down-induced flux expulsion and several possible values for the Ohmic decay time scale in the crust. In section **2.3,** implications of the adopted field decay model for the observed properties of single pulsars are explored assuming the same value for the field decay time scale in the crust of a neutron star as that inferred from our results from the binary evolution calculations. In section **2.4,** the adopted model for the spin evolution of neutron stars

in binary systems is described based on the discussions of chapter 1. The expected post-recycling behaviors of pulsars processed in binaries with companions of various masses are then considered while indicating specific cases corresponding to some of the observed systems.

2.3 Solitary Pulsars

If dipole magnetic field of neutron stars is assumed to decay exponentially with a time constant $\tau_{\rm Ohm}$ then Eq. 1.24 for the spin-down rate due to the dipole torque leads to

$$\dot{P} \propto e^{-\frac{2t}{\tau_{\rm Ohm}}} \tag{2.12}$$

which may be reduced to the form

$$\frac{\rm d}{{\rm d}t}\left(\frac{P_s}{P_0}\right)^2 = \frac{1}{t_0} e^{-\frac{2t}{\tau_{\rm Ohm}}} \tag{2.13}$$

where P_0 and t_0 are the spin period and the characteristic age of the pulsar ($t_{\rm sd} = \frac{P_s}{2\dot{P}_s}$) at birth (t = 0). Integrating this the time variation of the quantity $t_{\rm ch}$ may be found as

$$t_{\rm sd} = \left[t_0 + \frac{\tau_{\rm Ohm}}{2}\left(1 - e^{-\frac{2t}{\tau_{\rm Ohm}}}\right)\right] e^{\frac{2t}{\tau_{\rm Ohm}}} \tag{2.14}$$

which shows that for the case of exponential field decay the pulsar characteristic age $t_{\rm sd}$ grows exponentially with time and is much larger than the true age t. On the other hand for the case of the SIF model using $B_s(t) \propto \Omega(t)$ which is valid for times $t > \tau_{\rm Ohm}$ and assuming a spin-down rate due to the dipole torque (Eq. 2.6) it is predicted that at late times the magnetic field will decay very slowly as $B_s(t) \propto t^{-\frac{1}{4}}$, and the characteristic age is similar to the true age $t_{\rm sd}(t) \sim$ t (Srinivasan et. al. 1990).

The statistical properties of the population of *solitary* pulsars as implied by the SIF scenario would be quite different from that of a pure exponential field decay. By a pure exponential field decay model we mean one in which the whole magnetic flux within the star is assumed to decay exponentially, with no additional constraint. Considerations based on the computed evolutionary behavior and lifetimes of solitary pulsars prove in

fact to be very useful in this regard as discussed in the following. The results of these studies may be used to infer an effective value for the crustal decay time scale τ_{Ohm}.

The observed single pulsars have spin periods extending from 0.03 s up to $1-5$ s (see Fig. 2.1) which is believed to represent also the range of their spin evolution during a pulsar active lifetime (we do not consider the "millisecond pulsars" in the present context). According to the SIF model therefore a decay by a factor of $30-170$ in the surface field is expected for these pulsars during their lifetimes provided $t_{sd} > \tau_{Ohm}$ when they die: Although the predicted evolution of pulsars is in the beginning similar to that of a purely exponential field decay model, however the final *restricted* decay due to SIF has a distinct effect on the expected pulsar population. As is shown in Fig. 2.6a, the predicted paths of pulsars on the $B_s - P_s$ plane in general bend down (as in the exponential model) and extend vertically at an almost constant P_s, once $t_{sd} > \tau_{Ohm}$ is satisfied. However, if the vertical path does not cross the "death"-line which happens for an assumed value of $\tau_{Ohm} \lesssim 10^7$ yr for pulsars with a value of $B_i(G) \lesssim 10^{12.5}$, its subsequent evolution is expected to be along a track corresponding to a power-law dependence of the magnetic field on time, namely $B_s \propto t^{-\frac{1}{4}}$ (Srinivasan et al. 1990). During this period the decay of the field in the crust will keep pace with the expulsion of the flux which occurs with a time scale equal to t_{sd}, and no further substantial field decay will occur before the pulsar dies. The low-field pulsars would therefore experience a restricted field decay by less or an order of magnitude during their lifetimes and will populate the region with $B_s \lesssim 10^{11.5}$ G (Fig. 2.6a) in the observed pulsar population.

Consequently, the active lifetimes of these pulsar are predicted to be much larger than for the exponential model, or if one assumes no field decay at all during the pulsar lifetime. The theoretical determination of the active lifetime of a pulsar (ie. the time to cross the "death-line" in the $B_s - P_s$ plane) is based on the idea that the radio emission is due to charged particles which are produced in a gap in the magnetosphere of the star (see for example the review by Srinivasan 1989). The gap lies above the magnetic-polar cap and a potential difference of $\sim 10^{12}$ volts appears across it which is supported by the the potential difference between the poles and the equator of the

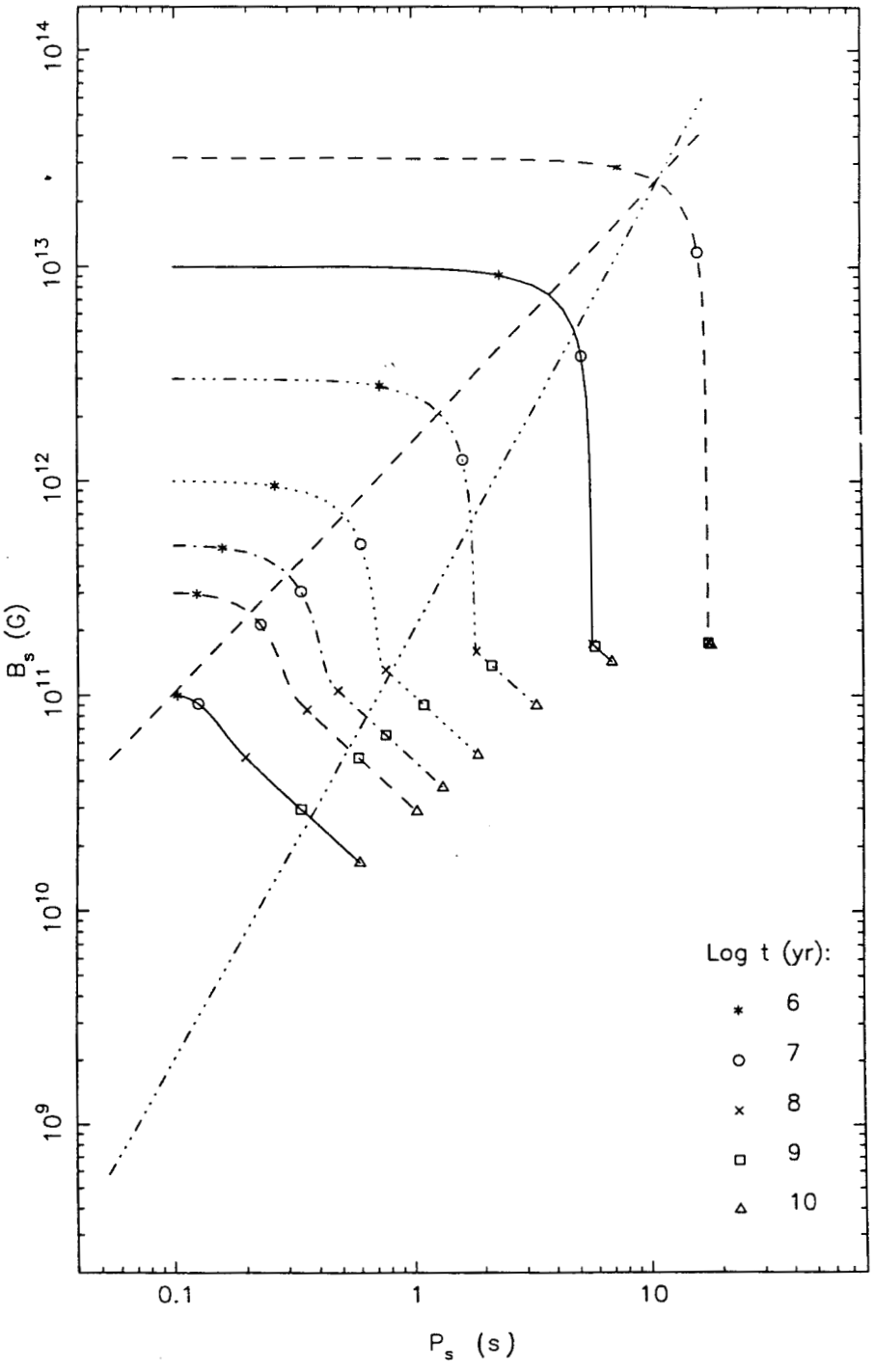

Figure 2.6(a)- Spin and magnetic field evolution of solitary pulsars born with the different assumed initial field strengths and a given initial period (= 0.1 s) are shown, according to predictions of the spin-down-induced flux expulsion scenario. Positions of the neutron stars at various ages are marked on each track, and the spin-up and death lines are also shown. **A** value of $\tau_{Ohm} = 10^7$ yr has been assumed.

pulsar which acts like a unipolar rotator (Goldreich & Julian 1969). The gap not only serves for the acceleration but also for generation of the charged particles namely electron-positron pairs. These are accelerated in the gap region along the magnetic field lines and produce very high energy 7-rays. The 7-ray photons in presence of the strong magnetic field in turn decay to new electron-positron pairs, the cycle is repeated and a cascade develops. In the pair creation model (Ruderman & Sutherland 1975) when the voltage generated by the pulsar (which is $\propto \frac{B_s}{P_s^2}$) drops below a critical value, copious pair production will cease and the pulsar will die. The radio-active lifetimes of pulsars will be hence computed using the condition $\frac{B_s}{P_s^2} = 0.2 \times 10^{12}$ (Chen & Ruderman 1993) which defines the death-line on the $B_s - P_s$ plane as shown in Fig. 2.1.

The predicted lifetimes of pulsars as defined above allowing for their spin-field evolution as in SIF are presented in Fig. 2.6b. The computed lifetimes of single pulsars with various values of B_i according to both SIF and the free exponential model are plotted for the different assumed values of $10^6 \leq \tau_{Ohm}(yr) \leq 10^9$. As expected Fig. 2.6b shows a marked increase in the lifetimes for those pulsars which undergo a restricted field decay predicted in the SIF model. The lifetimes of pulsars with comparatively large *initial* fields are seen in Fig. 2.6b to increase by an order of magnitude or less for the assumed values of $\tau_{Ohm} < 10^8$ yr according to SIF as compared to that expected if the field were to decay freely (marked as "Exp." on the figure) or not to decay at all. The latter case of no field decay may be judged from the behaviour of the curves for the larger values of τ_{Ohm} in Fig. 2.6b. The predicted increase in the lifetimes is obviously due to the decrease in the field values (as compared to the case of no decay) and that it does not result in a crossing of the "death-line" (in contrast to the free decay model). Furthermore, the increased lifetimes of the low-field pulsars are also seen to be larger for the smaller values of τ_{Ohm} in contrast to the behavior expected in the exponential model (Fig. 2.6b). The behavior and lifetimes of pulsars with large initial field strengths ($B_i \gtrsim 10^{12.5}$ G) are however the same for both models since they evolve along similar tracks until they cross the "death"-line.

The evolutionary behavior and the enhanced lifetimes of those solitary pulsars which

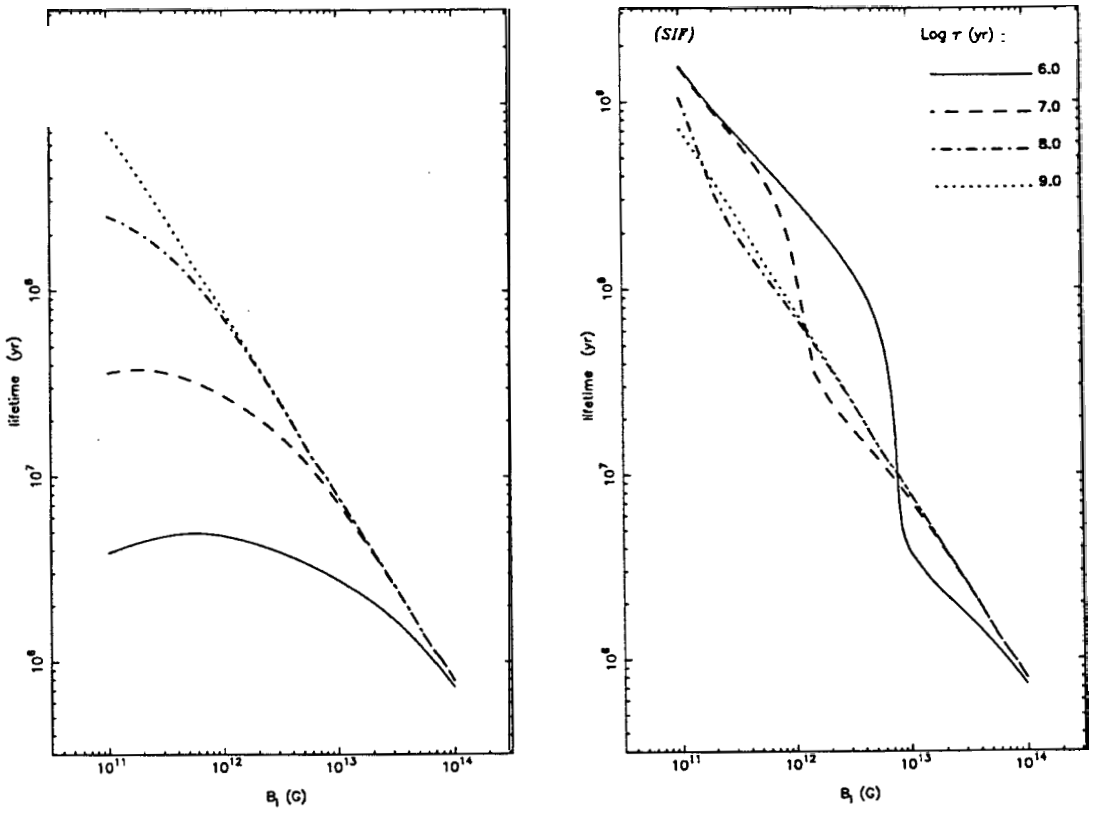

Figure 2.6(b)- The radio-active lifetime of pulsars versus the initial field strength B_i as predicted based on the spin-down-induced flux expulsion scenario scenario (SIF) and the pure exponential field decay model *(Exp.)*. Results for the different assumed values of the Ohmic time scale $\tau_{\rm Ohm}$ are shown in each panel by the different curves.

undergo a "restricted" field decay presented in Fig. 2.6a and Fig. 2.6b could account for the origin of the low-field ($B_s \lesssim 10^{11.5}$ G) pulsars which are observed to have only spin periods $P_s \gtrsim 0.5$ s. This would require, nevertheless, values of $\tau_{Ohm} \lesssim 10^7$ yr. The low-field pulsars could not have evolved from the extreme left and along constant field lines on the $B_s - P_s$ plane since that would imply a larger number of pulsars with periods $P_s < 0.5$ s to be observed at the lower than at the larger fields (Srinivasan 1991), in contradiction with the observed distribution of pulsars (cf. Fig. 2.1). The predicted downward motion (Fig. 2.6a) during the initial '(restricted" field decay phase could explain the evolution of these low-field pulsars from their initial small periods. In contrast to the majority of the solitary pulsars which have started their jouney on the $B_s - P_s$ plane from the extreme left ($P_s \lesssim 0.1$ s) of their present positions the low-field pulsars have started with similar short periods but at larger field values than their present fields. Also, the fact that members of this subset of pulsar population are found to have high altitudes above the galactic plane (Srinivasan 1991) would be still explained in terms of their old ages. This would also imply a magnetic-field–spatial-velocity correlation which favors the intermediate-age ($t_{sd} \sim 5 \times 10^7$ yr, for an assumed half oscillation time scale of $\sim 10^8$ yr about the Galactic plane) low-field pulsars, being at larger heights above the plane, to have lower velocities due to the gravitational deceleration acting on them during their journey from their birth places in the Galactic plane.

2.3.1 **Population** Synthesis

Statistical studies of the single pulsar population suggest values of the field decay time scale ranging from $\lesssim 10^7$ yr up to $\gtrsim 10^8$ yr (eg. Narayan & Ostriker 1990; Bhattacharya et al. 1992). In all these studies the pulsar surface magnetic field has been however assumed to decay "freely" with an exponential or a power-law time-dependence. Although a similar exercise has to be repeated in order to see how the results of such studies would be modified for the case of the SIF model of field decay, the following argument seems to be supported by the implications of the earlier studies.

Monte Carlo simulations of the observed properties of pulsars which have preferred values of $\tau_{Ohm} \gtrsim 10^8$ yr are however expected to imply a lower value of $\tau_{Ohm} \sim 10^7$ yr if a sample of pulsars with initial long periods and low field strengths is further included in the adopted population (Bhattacharya et al. 1992). Similar low values of the decay time scale have been also inferred from a different study in which a second generation of pulsars (assumed to be born at large heights above the galactic plane and with low initial magnetic fields) has been also considered in addition to the pulsars born in the Glactic plane (Narayan & Ostriker 1990).

The restricted field decay predicted in the SIF model for an assumed value of $\tau_{Ohm} \sim 10^7$ yr would on the other hand have the effect of increasing in the population of long-lived low-field single pulsars, as discussed earlier. Simulation of a single disk population of pulsars with an assumed value of $\tau_{Ohm} \sim 10^7$ yr might be therefore expected to be consistent with the statistical properties of the observed pulsars if magnetic fields are assumed to evolve according to the SIF model.

2.4 Recycled Pulsars

2.4.1 Description of the Computations

Next we consider models for the orbital and spin evolution of a newborn neutron star in a binary with an orbital period P_{orb} with a mainsequence star of mass M_2 which loses mass in the form of a spherical uniform stellar wind at a rate $\dot{M}_2$. In the picture of spin-down-induced field expulsion the evolutions of the spin period and the magnetic field of the neutron star in such a binary would be intimately coupled. While the spin-down process would tend to reduce the field strength, the reduced field strength (together with the increased spin period) will in turn affect the rate and the direction of the spin variations. *We follow this coupled evolution of the surface magnetic field and the spin period of the neutron star for a time equal to the expected mainsequence lifetime of the companion star.* The computations are, however, stopped if a Roche-lobe overflow is indicated at some stage during this period.

In accord with the discussions in chapter 1, we assume that the first phase of the evolution, namely the pulsar phase with a dipole spin-down (during which the neutron star spins down due only to the dipolar radiation torque on it), lasts till the ram pressure of the stellar wind overcomes the pressure of the "pulsar wind" at the accretion radius (see, e.g., Illarionov & Sunyaev 1975; Davies & Pringle 1981). During this period the stellar wind will have no dynamical effect on the neutron star. The pulsar's core magnetic field will undergo an expulsion determined by the dipole spin-down rate. In the subsequent phases where the accreted wind matter interacts directly with the magnetosphere we assume that a steady Keplerian disk is formed by the accretion flow outside the magnetosphere, with the same sense of rotation as that of the neutron star. This is the least efficient configuration for angular momentum extraction from the neutron star. More efficient geometries such as a spherically symmetric radial infall may well occur for the low mass accretion rates appropriate to these objects (Hunt 1971; Illarionov & Sunyaev 1975; Wang 1981). Therefore we also explore a few cases corresponding to a radial infall on the neutron star for comparison.

We note, however, that the sign, magnitude, and time-dependence of the accretion torque produced by capture of plasma from a stellar wind is a complex problem that has only partially been solved (Ghosh & Lamb 1991) and the outcome depends on the detailed properties of the flow at the capture radius which determine the feasibility of formation of an accretion disk (Ho & Arons 1987; Taam, Fu & Fryxell 1991). Also, a second difficulty lies in the fact that even in the case where a disk is formed uncertainties in the nature of interaction of the magnetosphere of the neutron star with the wind plasma have led to widely different predictions for the accretion torque on the neutron star (Holloway, Kundt & Wang 1978; Kundt 1990; Ghosh & Lamb 1991).

Confronted with the need of a simple and specific model for the spin evolution of the neutron star, we have decided to adopt the following description drawn from the models commonly encountered in the literature (see, e.g., Pringle & Rees 1972; Illarionov & Sunyaev 1975). The accretion flow interacts with the magnetosphere at the so-called Alfvén or the magnetosphere radius $R_{\rm mag}$ (cf. Eq. 1.19; see also Eq. 1.21 and the related discussion):

$$R_{\rm mag} = 7.03 \times 10^{-8} \left(\frac{B_8^2}{\dot{M}_{\rm acc}}\right)^{2/7} R_\odot \qquad (2.15)$$

where B_8 denotes the surface field strength in units of 10^8 gauss and $\dot{M}_{\rm acc}$ the rate of capture of wind matter in solar masses per year (Davidson & Ostriker 1973). This interaction spins the neutron star up or down depending on the sign of the quantity $V_{\rm dif}(= V_{\rm corot} - V_{\rm Kep})$ evaluated at the radius of the magnetosphere. Here, $V_{\rm corot}$ is the speed of co-rotation with the neutron star at a given distance from it, and $V_{\rm Kep}$ is the Keplerian speed at the same distance. The boundary is determined by the condition of balance between the magnetic pressure and the ram pressure of the infalling flow. In the limiting case when the co-rotation velocity $V_{\rm corot}$ becomes equal to the Keplerian velocity $V_{\rm Kep}$ the neutron star will conserve its spin period while accretion onto the star will continue. The rate of transfer of angular momentum between the stellar wind and the neutron star $\dot{L}_{\rm s}$ is assumed to be equal to $\dot{M}_{\rm acc}$ times a specific angular momentum corresponding to the difference between the co-rotation velocity with the neutron star and the Keplerian velocity around it at the radius of its magnetosphere boundary (d.

Eq. 1.30). In general then

$$\dot{L}_s = \xi \times V_{dif} \times R_{mag} \times \dot{M}_{acc} \qquad (2.16)$$

will be used, where ξ is the efficiency factor included to take into account the uncertainties due to the detailed geometry of the interaction and the actual value of the specific angular momentum carried by the accreted wind just before and after the interaction. Different rates of angular momentum transfer are thus tested by assuming different values for ξ while $\xi = 1$ corresponds to the case of disk-accretion with a mechanical torque acting at R_{mag} (cf. § 1.4.3).

The amount of spin angular momentum added to, or extracted from, the neutron star (and loss in mass and angular momentum of the system) is calculated by assuming that:

a) in the "propeller" phase all of the accreted matter is expelled by the magnetosphere and leaves the system at the Alfvén radius with no further interaction, carrying a total orbital angular momentum corresponding to its co-rotation with the neutron star, as is the case for a "weak" wind (Holloway et al. 1978); and

b) in the accretion phase all of the accreted matter enters the magnetosphere carrying with it only the excess spin angular momentum due to the difference between the Keplerian and co-rotation angular velocities.

The fraction of the stellar wind which does not enter the accretion flow towards the neutron star is assumed to escape from the binary system with a specific angular momentum equal to that of the secondary star. The coefficients α and β in eq. 2.15 for the orbital evolution are computed based on these assumptions as discussed in § 1.5 (cf. Eqs 1.41, 1.42, and 1.43). The accretion rate M_{acc} is affected by the variation of a (the orbital separation). The instantaneous values of $\dot{M}_{acc}$ and B_s determine the magnetospheric or the Alfvén radius R_{mag}. The residual magnetic field B_f (cf. Eq. 2.10 and Fig. 1.2) which corresponds to the amount of magnetic flux still trapped in the stellar core is assumed to decrease in proportion to an increase in the spin period P_s *instantaneously* (Eq. 2.8). The surface field B_s then approaches B_f exponentially with

a constant decay time scale $\tau_{\rm Ohm}$. At the start of the evolution $B_{\rm c}$ and $B_{\rm s}$ are set to be equal.

The coupled differential equations for time evolution of $M_{\rm n}$, a, $P_{\rm s}$, $B_{\rm c}$, and $B_{\rm s}$ which are listed below are integrated numerically using a fourth-order Runge-Kutta scheme, for various sets of parameters.

$$\frac{{\rm d}a}{{\rm d}t} = 2a\left\{\frac{\dot{L}_{\rm losses}}{L_{\rm orb}}\Big|_{\rm losses} - \frac{\dot{M}_2}{M_2}\left[1 + (\alpha - 1)\frac{M_2}{M_{\rm n}} - \frac{1}{2}\alpha\frac{M_2}{M} - \alpha\beta\frac{M_{\rm n}}{M}\right]\right\} \quad (2.17)$$

$$\frac{{\rm d}M_{\rm n}}{{\rm d}t} = \begin{cases} \dot{M}_{\rm acc} & \ldots\ldots\ldots\ldots \text{ accretion phase} \\ 0.0 & \ldots\ldots\ldots\ldots \text{ propeller phase} \end{cases} \quad (2.18)$$

$$\frac{{\rm d}P_{\rm s}}{{\rm d}t} = 3.18 \times 10^{-3}\,\xi\left(\frac{M_{\rm acc}}{M_\odot/{\rm yr}}\right)\left(\frac{R_{\rm mag}}{\rm km}\right)\left(\frac{P_{\rm s}}{\rm sec}\right)^2\left(\frac{V_{\rm dif}}{\rm km/sec}\right)\ {\rm s\ yr^{-1}} \quad (2.19)$$

$$\frac{{\rm d}B_{\rm c}}{{\rm d}t} = \begin{cases} -(\dot{P}_{\rm s} \times B_{\rm c})/P_{\rm s} & \ldots\ldots\ldots \text{ if } \dot{P}_{\rm s} > 0.0 \\ 0.0 & \ldots\ldots\ldots\ldots \text{ otherwise} \end{cases} \quad (2.20)$$

$$\frac{{\rm d}B_{\rm s}}{{\rm d}t} = -\frac{(B_{\rm s} - B_{\rm c})}{\tau_{\rm Ohm}({\rm yr})} \quad (2.21)$$

where $L_{\rm orb}$ is the orbital angular momentum, $L_{\rm losses}$ is the rate of change in $L_{\rm orb}$ except for that due to escaping matter from the system, M is the total mass of the binary, a is the ratio of the mass loss rate from the system to that from the secondary, and β is the ratio of the effective specific angular momentum of the escaping matter to that of the secondary star. Note that during the active pulsar phase $\dot{P}_{\rm s}$ will be given by **Eq.** 1.26 instead of **Eq.** 2.19 which is applicable for the last two evolutionary phases.

2.4.2 Low-mass Progenitors

In the study of X-ray binaries, accretion from the stellar wind of the companion is usually invoked only in the case of High Mass X-ray Binaries (HMXBs) (van den Heuvel 1981; Henrichs 1983). This is so because in the case of low-mass binaries wind accretion will not be able to produce a perceptible X-ray emission. *This feeble stellar wind in low-mass binaries is nevertheless the key factor responsible for the spinning-*

down of the neutron star. The long mainsequence lifetime of the low-mass donor allows for the long (up to a few times 10^9 yr) spin-down (dipole and propeller) phases. In view of the lack of observational data, as well as theoretical predictions of mass loss rates of dwarf mainsequence stars (see, e.g., Dupree 1986; de Jager, Nieuwenhuijzen & van der Hucht 1988; Chiosi, Bertelli & Bressan 1992), we use values both larger and smaller than the observed mass loss rate of the sun, namely $2 \times 10^{-14}\ M_\odot/\mathrm{yr}$ (Cassinelli 1979). In the case of "wide" low-mass binaries in which we are primarily interested here, the orbital separation a of the binary remains almost constant during the wind phase since the angular momentum losses due to the gravitational radiation and magnetic braking are very inefficient. However, we do take into account the effects of angular momentum loss, as well as the loss and exchange of matter in computing the orbital evolution during this phase. As is borne out by our calculations, the flux expulsion occurs entirely during the detached phase of the binaries. In wide low-mass binaries (with orbital periods more than a day) the duration of the detached phase is nearly equal to the mainsequence lifetime of the donor. We confine ourselves to only such systems so as to avoid computing the duration of the detached phase resulting from the highly uncertain degree of magnetic braking in binaries with shorter periods.

We follow the evolution of the system over a period of 10^{10} years which is of the same order as the mainsequence lifetimes of solar type stars (Schallar et al. 1992). Fig. 2.7a displays the typical evolutionary behavior observed for the spin period and the residual and surface magnetic fields of the neutron star in our models. The values of the spin period following its maximum are somewhat less reliable for the reasons mentioned above. The spin-up phase considered here is only due to the accretion from the stellar wind of the companion and will be succeeded by a much more enhanced accretion phase when Roche-lobe overflow ensues during the post-mainsequence evolution of the donor. The spin evolutions of neutron stars in binaries with different orbital periods are compared in Fig. 2.7b. The time elapsed before the transition of the binary into the "propeller" phase ranger between 10^8 to 3×10^9 yr (larger P_{orb} and/or lower $\dot{M}_2$ result in larger values for the elapsed time) in different models (Fig. 2.7b). During this

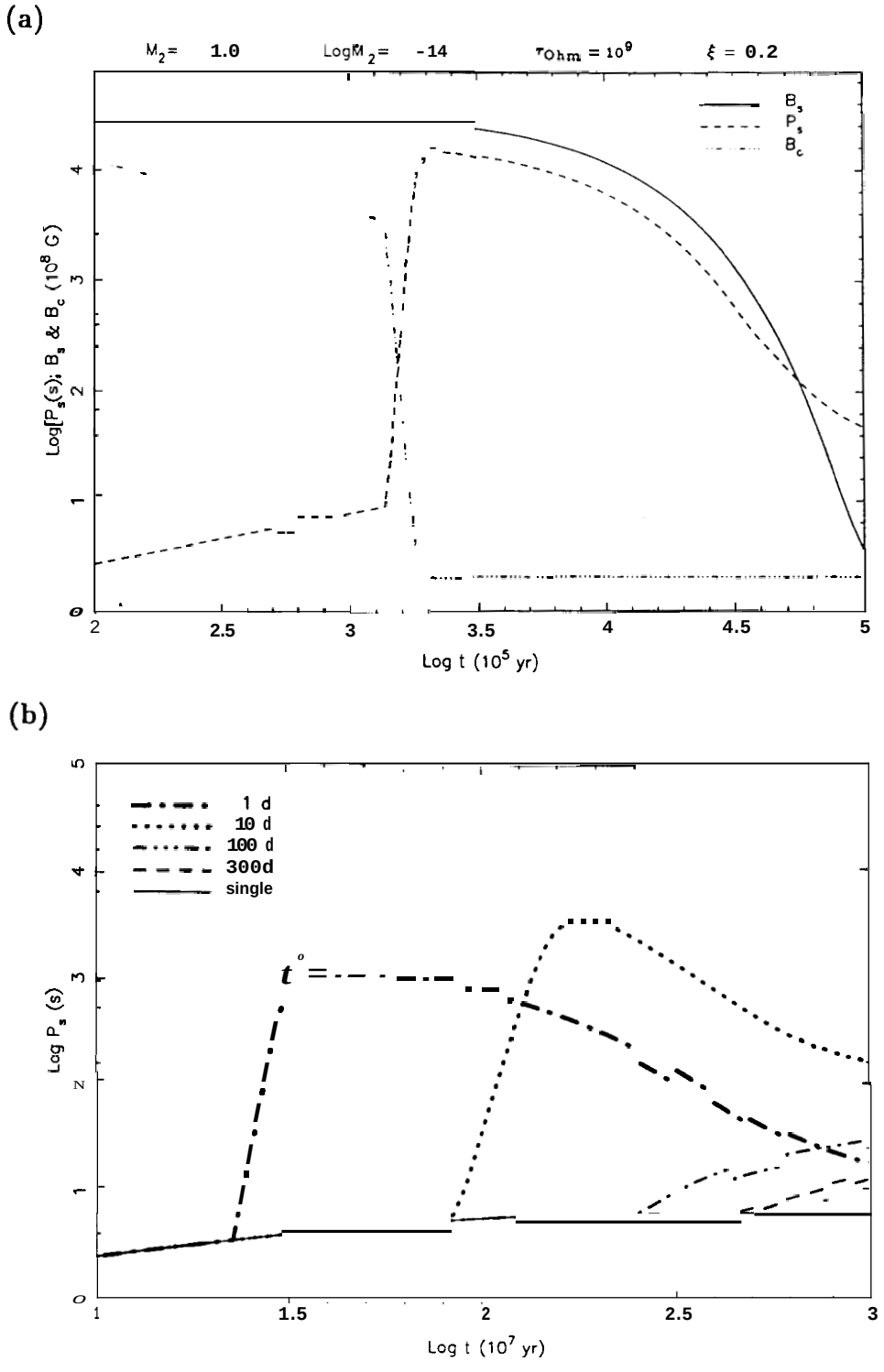

Figure 2.7- (a) Evolution of the spin period P_s, and the magnetic field strength in the core B_c and at the surface B_s of a neutron star in a low-mass binary, according to the spin-down-induced flux expulsion scenario. M_2 is the companion mass in solar masses, $\dot{M}_2$ is the wind rate of the companion star in $M_\odot$/yr, τ_{Ohm} is the Ohmic decay time scale in the crust in yr, and ξ is an efficiency factor that determines the degree of angular momentum transfer in the magnetosphere–wind interaction. The initial orbital period of the binary has been assumed to be 3 d. **(b)** Spin evolution of neutron stars in binaries with different initial orbital periods (1, 10, 100 and 300 days), and that of a solitary pulsar. Initial values of $P_s = 0.4$ sec, and $B_c = B_s = 10^{12}$ G have been used. M_2, $\dot{M}_2$, τ_{Ohm} and ξ are the same as in **(a).** [from Jahan Miri & Bhattacharya 1994]

period the neutron star is assumed to spin down at a small rate due only to a dipole radiation torque similar to an isolated pulsar (Eq. 1.26). The case of a 10^{10} yr pure dipole phase (same as that of a solitary pulsar) has also been included. This happens in very wide binaries where the pressure of the accreted matter can never overcome the radiation pressure of the pulsar (which gives rise to the flat portion seen in some of the curves in Fig. 2.8 below). The propeller phase on the other hand lasts for $\sim 10^7$–3×10^8 yr depending on the value of the efficiency factor ξ.

The longest spin periods obtained are of the order of a few times 10^4 s which result in final field strengths of $\sim 10^8$ G, while spin periods of ~ 1000 s result in a value of $\sim 10^9$ G for the final strength of the surface field. These long spin periods seem reasonable in view of the long periods observed in some X-ray pulsars (the largest known value being ~ 835 sec; see, e.g., Nagase 1989). Fig. 2.8 shows the final surface field strengths B_s obtained for models with orbital periods between 1 to 400 days, for the given values of the parameters. These have been selected from a larger sample of computed models which cover the following range of parameters and initial conditions:

ξ: 0.02, 0.1, 0.2, 0.6, 1, 10,100	
M_2: 0.8, 1.0	($M_\odot$)
$\log \tau_{\rm Ohm}$: 7.0, 8.0, 9.0	(yr)
$\log \dot{M}_2$: −16, −15, −14, −13	($M_\odot$/yr)
initial P_s: 0.1, 0.4, 1.0	(sec)
V_w: 400, 600, 800	(km/sec)
initial B_s: 10^{12}, 3 x 10^{12}, 10^{13}	(G)

In Fig. 2.8 we restrict ourselves to values of $\xi \lesssim 1$; the results for the much larger values of $\xi \gtrsim 10$ will be presented separately below. The initial spin period of a neutron star is an important factor for deciding its magnetic field evolution according to the SIF model. Very short spin periods $\sim 10^{-3}$ s have been assumed by some authors (Ding, Cheng & Chau 1993) in a study of similar nature as the present work (see chapter 3). However, it is not at all clear that neutron stars are indeed born with such short periods. For the Crab pulsar the estimated initial period is ~ 20 ms (Trimble & Rees

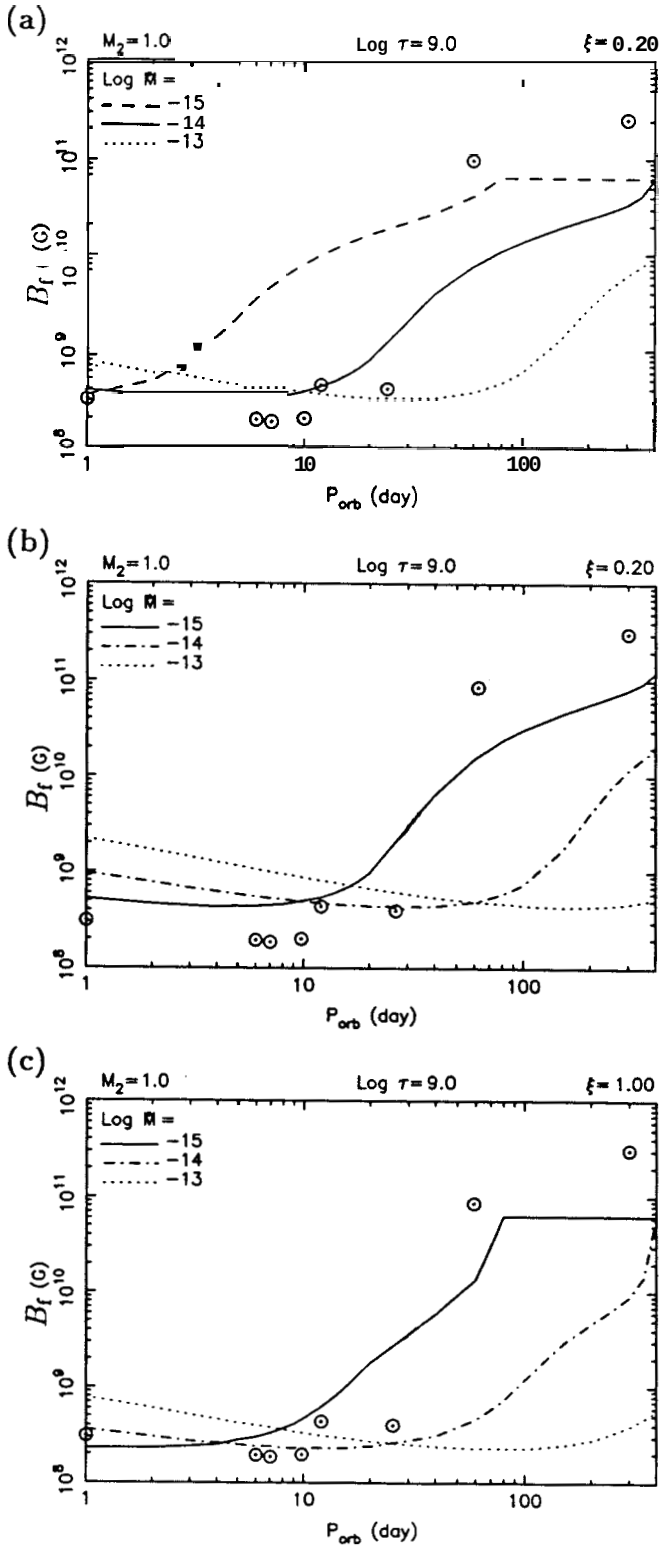

Figure 2.8- Final values of the surface magnetic field strengths B_f of neutron stars evolved in binaries with various orbital periods P_{orb} and mass loss rates $\dot{M}$. Encircled dots represent observed binary radio pulsars that are descendants of wide low-mass binaries, for which the initial orbital periods can be estimated. See the caption of Fig. 2.7a for explanation of the legends. (a) The assumed values of parameters and initial spin periods and magnetic fields of the neutron stars are the same as for Fig. 2.7b. **(b)** Same as (a), but for initial $P_s = 1.0$ s, and $B_c = B_s = 3 \times 10^{12}$ G. ***(c)*** Same as (a), but for a different efficiency factor: $\xi = 1.0$. [from Jahan Miri & Bhattacharya 1994]

1970). Absence of a large number of bright center-filled supernova remnants indicate that most pulsars are born with spin periods much exceeding $\sim$ 20 ms (Srinivasan, Bhattacharya & Dwarakanath 1984). Statistical studies of pulsar population have also found evidence for the majority of pulsars being born with periods exceeding $\sim$ 100 ms (Vivekanand & Narayan 1981; Chevalier & Emmering 1986; Narayan 1987; Emmering & Chevalier 1989; Narayan & Ostriker 1990).

The two sets of initial values used for the spin periods and magnetic field strengths in the models presented in Figs 2.8a & b correspond approximately to the extreme values observed in young radio pulsars. We assume that the initial values of spin period and field strength of a neutron star born in a binary are independent of its orbital period, since no mechanism is known so far which would result in a correlation between these quantities.

Variations in the efficiency factor ξ affect the final results in the same way as the variations in the mass loss rate, and the best correspondence with observations appears to result from a $\xi \dot{M}_2 \sim 10^{-15}\ M_\odot/\mathrm{yr}$. The variations in final results due to the changes in ξ ($\lesssim 1$,; the effects due to the much larger values are discussed later on) are however not very large; compare Figs 2.8a & c. Therefore, in spite of the fairly crude physical model which has been used, and the existing uncertainties in the nature of the captured flow and the details of the magnetospheric interaction with the accreted plasma, the results presented here can be safely used as a good indicator of what is expected from the spin-down-induced magnetic field decay mechanism.

The final magnetic fields that result from the models presented in Fig. 2.8 are in broad agreement with the observed fields in the millisecond and other recycled pulsars. The circles in Fig. 2.8 represent eight observed low-mass binary radio pulsars which are listed in Table 2.1 along with some of their properties. These are believed to be the only known descendants of disk-population "wide" LMXBs for which the initial orbital periods can be estimated with reasonable confidence. In these binaries the total mass is assumed to be almost conserved throughout the evolution and the initial and final

values of the orbital period $P_{\rm orb}$ are related as

$$\frac{P_{\rm orb-0}}{P_{\rm orb-\infty}} = \left(\frac{M_{1-\infty}\, M_{2-\infty}}{M_{1-0}\, M_{2-0}}\right)^3 \qquad (2.22)$$

where -0 and $-\infty$ subscripts denote the initial and final values of the respected quantity. While the orbital period of such an X-ray binary increases during its final evolutionary phase of Roche-lobe overflow it remains almost constant throughout its earlier stellar-wind mass-transfer phase. Therefore the mainsequence lifetime of the donor is spent within a detached binary.

Table 2.1- The observed low-mass binary pulsars

PSR	P_s (msec)	$P_{\rm orb}$ (day)	M_2 ($M_\odot$)	$\log B_s$ (G)	initial $P^*_{\rm orb}$ (day)
0820+02	864	1232	0.2–0.4	11.48	300
1953+29	6.13	117	0.2–0.4	8.63	12
1855+09	5.36	12.3	0.2–0.4	8.48	1
J1713+0747	4.57	67.83	0.3–0.5	8.28	6
J2019+2425	3.93	76.51	0.3–0.5	8.26	7
J1643−1224	4.6	147	0.14	8.6	24
J1455−3330	8.0	76	0.3	8.3	10
B1800−27	334.4	406.8	0.15	10.9	60

References: Bhattacharya and van den Heuvel 1991
Foster, Wolszczan and Camilo 1993
Nice, Taylor and Fruchter 1993
Johnston et al. 1995; Lorimer et al. 1995a

*As estimated from evolutionary models, using Eq. 2.22

As can be seen from Table 2.1 and Fig. 2.8, the surface magnetic field of PSR 0820+02 (3×10^{11} G) is much larger than what is obtained in any of our calculated models, even though the evolution of the model-binaries with orbital periods of $\gtrsim 300$ days is entirely governed by the spin-down due to a dipole torque. Since a value of $\tau_{\rm Ohm} =$

10^9 yr is favored by our results *for choices* of $\xi \lesssim 1$, the large field strength of PSR 0820 + 02 could be explained (in the case of small values of ξ) if the age of the neutron star is not more than $\sim 4 \times 10^9$ yr, which may happen if either the donor star had a mass somewhat higher than 1 $M_\odot$ or the neutron star was born in an accretion-induced collapse (AIC) of a white dwarf. Note, however, that our results for the assumed values of $\xi \gtrsim 10$, which are discussed later on in this section, the predictions are in good agreement with the observed field of PSR 0820 + 02, as well as with the other sources (cf. Fig. 2.9 below). Nevertheless, Fig. 2.8 shows that the adopted model is successful in reproducing the observed magnetic fields of most of the pulsars which are believed to have been recycled in wide low-mass binaries, as well as the apparent relation between the final field strength and the initial orbital period, a possibility which has not been shown to exist in any other scenario.

Such a relation between the final field strengths and the initial orbital periods has not been shown explicitly to exist for any other field decay model. The model of field decay by mass accretion which claims to be successful in reproducing the general distribution of the recycled pulsars in the B_s—P_s diagram (Romani 1990), seems to have difficulty in at least one example: the neutron star in 4U1626 − 67 has a strong magnetic field of $\sim 10^{12}$ G, although it is expected to have accreted a large amount of mass and hence should have a weak field on that account (Verbunt, Wijers & Burm 1990). However, in the picture presented here the high magnetic field of this neutron star at present seems to be a natural consequence of its evolutionary history. As described by Verbunt et al. (1990), there could have been two evolutionary paths leading to this system. One in which the neutron star is formed via AIC of a white dwarf accreting from a ~ 0.02 $M_\odot$ degenerate donor; in which case obviously the phase of stellar wind interaction is absent and thus the amount of field expulsion is low. In the second case where the AIC happens due to accretion from a $\gtrsim 0.1$ $M_\odot$ mainsequence star, our computations show that the neutron star would retain a high magnetic field unless the wind from the donor exceeds a rate of 10^{-14} $M_\odot$/yr, which is unlikely for a star with such a low-mass. In addition, it is important to note that the various

mechanisms discussed in the context of accretion-induced field decay in neutron stars [amely: i)-reduction in the conductivity due to heating of the crust, ii)-compression of the current carrying layers, and iii)-inverse thermoelectric battery effect] can destroy or modify the magnetic flux *confined to only the crust.* All these effects are however unlikely to have any significant influence on the field that resides in the core of the star. The accreted plasma might be able to temporarily screen the interior field and reduce the strength of the surface field, but the field would resurface if the flux resides in the core (Bhattacharya & Srinivasan 1993).

Nevertheless the accretion-induced field decay could play a major role in the field history of some neutron stars recycled in binary systems provided the spin-down-induced field decay is also operative. This comes about as the latter mechanism brings the field up to the crust which could be then killed more quickly than expected for the normal decay time scale τ_{Ohm} of the crust during an efficient accretion phase in the binary. Such a cooperative field decay due to the two processes was already invoked in § 2.1.1 in order to resolve the issue regarding the observed field strengths of the X-ray pulsars versus that of the recycled radio pulsars. It will be further discussed in § 2.4.3 (referred to as a *temporary* reduction in the Ohmic decay time scale of the crust; see also Table 2.5) when the predictions of the SIF model for the post-recycling behavior of pulsars descending from massive binaries are explained.

Effects of the Crust:

i) Decay time scale

Final field strengths as low as $\sim 10^8$ G are obtained only if the Ohmic time scale τ_{Ohm} lies in the range $10^{8.5} - 10^9$ yr. If τ_{Ohm} is lower than this then the spin-down stops too soon and not enough flux is expelled. For $\tau_{Ohm} \gtrsim 10^9$ yr on the other hand the surface field does not have time to decay to $\sim 10^8$ G in a Hubble time. It should be noted that values of $\tau_{Ohm} \sim 10^9$ yr are shorter than that has been computed for pure matter at the *bottom* of the crust (Baym, Pethick & Pines 1969; Sang & Chanmugam 1987). However, it is by no means clear to what extent the crustal matter of a neutron

star is an ideal lattice. It has been shown that even a small amount of impurities and dislocations can drastically reduce the Ohmic time scale (Yakovlev & Urpin 1980; Urpin & Van Riper 1993; Bhattacharya & Datta 1996). Furthermore, the expelled field may eventually undergo a turbulent cascade which would also bring the effective Ohmic time scale down (Goldreich & Reisenegger 1992).

As discussed earlier (§ 2.2.2), the evolution of pulsars recycled in binary systems with lifetimes much larger than $\tau_{\rm Ohm}$ (namely LMBPs) are determined only by their maximum spin period $P_{\rm max}$ values (see Eq. 2.10 and Fig. 1.2). Hence, it might seem unnecessary to inspect the properties of pulsars recycled in low-mass systems in order to infer any constraint on the value of $\tau_{\rm Ohm}$ provided that a value of $\tau_{\rm Ohm} >$ few$\times 10^9$ yr is not considered to be relevant at all. However, even in the case of these binaries it turns out that the predicted behavior of the recycled pulsars do depend on the assumed value of $\tau_{\rm Ohm}$ *through its effect on the value of* $P_{\rm max}$. *A* value of $10^8 \lesssim \tau_{\rm Ohm} \lesssim 10^9$ yr is suggested by the results of model computations for the low-mass systems, provided $\xi \lesssim 1$ (Fig. 2.8).

Nevertheless, values as low as $\tau_{\rm Ohm} \sim 10^7$ yr could produce acceptable results for the simulations of LMBPs provided a more efficient spin-down mechanism with associated values of $\xi \gtrsim 10$ is considered. The results for smaller values of $\tau_{\rm Ohm}$ are shown in Fig. 2.9 where larger values of ξ have been used than in Fig. 2.8. It is important to note that in addition to the dependence of the final field values on the assumed values of the mass-loss rate of the companion (indicated by the different curves in Figs 2.8 & 2.9), the initial values of the pulsar spin period and field strength as well as the velocity of the stellar wind also have a significant effect on the predicted final field values in both Figs 2.8 & 2.9. *One should also bear in mind that these quantities need not have the same value for all pulsars and all binaries* !. Also notice that as indicated above for values of $\tau_{\rm Ohm} \sim 10^7$ yr larger values have to be assumed for the efficiency factor ξ than in the case of $\tau_{\rm Ohm} \gtrsim 10^8$ yr (compare Fig. 2.8 with Fig. 2.9). Large values of $\xi >> 1$ might be in fact expected to be the case because the rate of angular momentum transfer during a "propeller" phase corresponding to an assumed value of $\xi = 1$ is indeed the

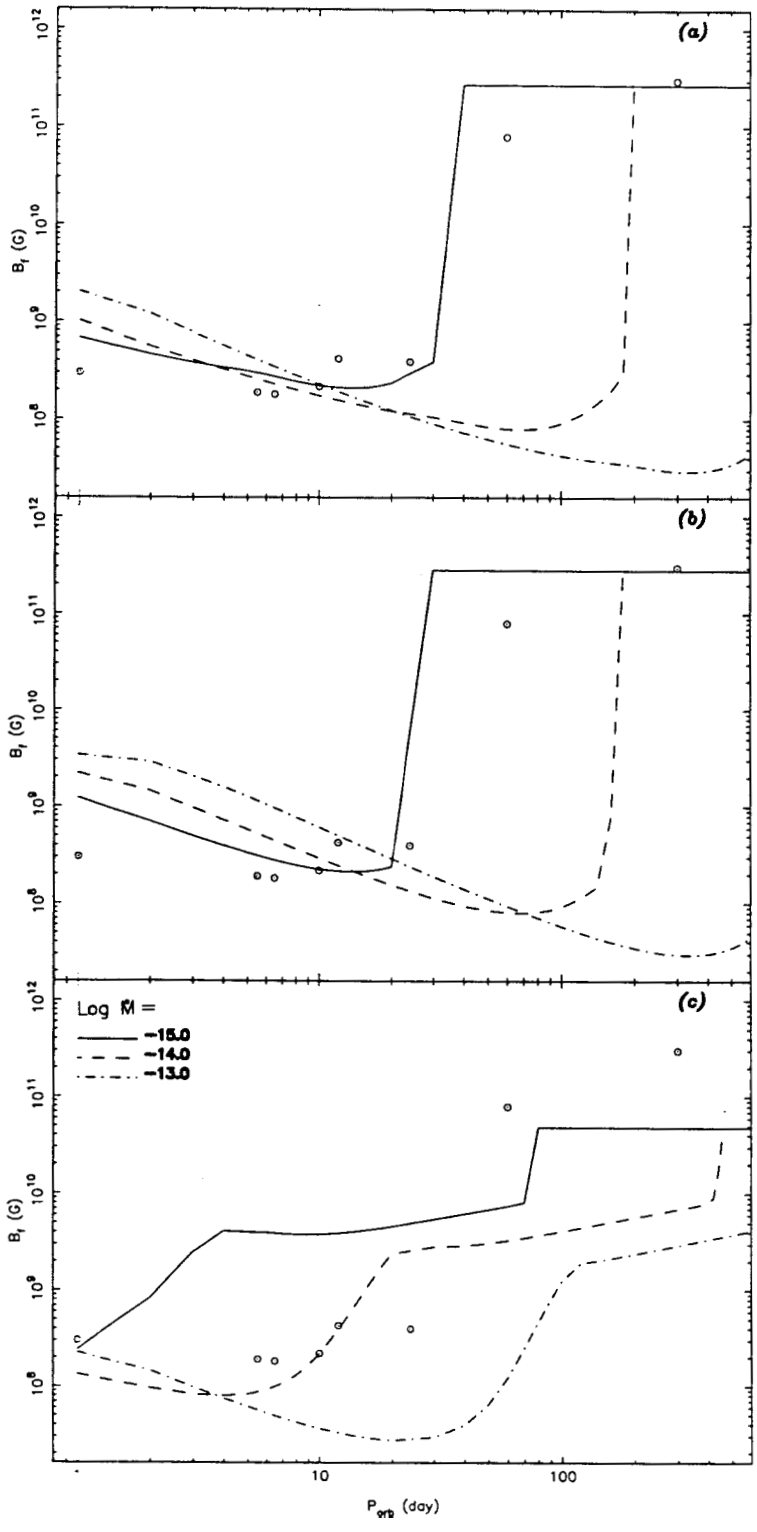

Figure **2.9**- Same as Fig. 2.8a, but for smaller values of the decay time scale $\tau_{\rm Ohm}$, larger values of the efficiency factor ξ, and the indicated initial spin periods P_{s-0} : *(a)* for $\tau_{\rm Ohm} = 10^8$ yr, $\xi = 10$, and $P_{s-0} = 1$ s, (b) for $\tau_{\rm Ohm} = 10^7$ yr, $\xi = 100$, and $P_{s-0} = 1$ s, and *(c)* for $\tau_{\rm Ohm} = 10^8$ yr, $\xi = 1$, and $P_{s-0} = 0.1$ s.

least efficient one among the models discussed in the literature (Wang 1981) as noted earlier (cf. § 1.4). Fig. 2.9 shows that the observed distribution of fields in old recycled pulsars with low-mass companions may be accounted for by SIF for assumed values of $\tau_{\rm Ohm} << 10^9$ yr provided $\xi >> 1$. In fact the agreement between the predictions and the observational data seems to be even better for the smaller values of $\tau_{\rm Ohm}$ as in Fig. 2.9 than for the cases with larger values of $\tau_{\rm Ohm}$ as in Fig. 2.8. We are inclined to infer a value of $\tau_{\rm Ohm} \sim 10^{7.5}$ yr from these results.

Short time scales $\lesssim 10^7$ yr for field decay of pulsars have been indeed suggested by different observational investigations (Gunn & Ostriker 1970; Lyne, Manchester & Taylor 1985; Narayan & Ostriker 1990). Also theoretical studies of the field decay in the crust of neutron stars, being subject to uncertainties regarding the correct value of the electrical conductivity of the crustal matter as well as the effects of the unknown geometry and boundary conditions of the field distribution have resulted in a large range of values for the decay time scale, which nevertheless extends to values as low as few Myr (Flowers & Ruderman 1977; Muslimov & Tsygan 1985; Jones 1987; Jones 1988; Wendell 1988; Sang & Chanmugam 1990; Bhattacharya & Datta 1996).

ii) Boundary effects

The assumption of instantaneous expulsion of the magnetic flux out of the superconducting core of a neutron star in response to an increase in the spin period of the star is, of course, viable only when flux can move freely across the core-crust interface. It has however been pointed out by Jones (1987) that once the flux density in the solid reaches a value of $\gtrsim H_{c1}$, the lower critical field of the proton superconductor, further transport of flux across the boundary is hindered, and a layer of high fluxoid density builds up just below the border. From then on flux is released into the solid in the same time scale in which flux transport occurs in the solid crust – by Ohmic diffusion, Hall transport or plastic flow.

Estimates of the mechanical strength of the crust suggest that plastic flow might become the major means of flux transport well before the field in the solid builds up

to H_{c1} (Ruderman 1991b). The critical strain at the bottom of the crust, estimated to be $\lesssim 10^{-3}$ (Ruderman 1991a, Baym & Pines 1971, Smoluchowski 1970), implies that the maximum magnetic stress that can be sustained in this region is several orders of magnitude less than $H_{c1}^2/8\pi$ (Jones 1987). As long as the time scale for spin-down is longer than that for plastic flow, flux will thus move more or less freely across the core-crust interface. If the plastic flow time scale is $\lesssim 10^6$ yr, as estimated by Jones (1987), nearly all of our models will operate in this regime and hence the assumed instantaneous response could be justified.

Nevertheless, since uncertainties in the above numbers are large, we have also examined a few models in which the flux flow across the interface is determined by Ohmic diffusion of flux in the solid, and the time scale of flux transfer from superfluid to the solid is set equal to the assumed Ohmic time scale right from the beginning of evolution (this overestimates the effect of the hindrance to flux expulsion) in order to gauge the impact of this on our results. The evolution of core field B_c is calculated in this case from

$$\dot{B}_{res} = -\dot{P}_s \frac{B_{res}}{P_s} \tag{2.23}$$

$$\dot{B}_c = \frac{B_c - B_{res}}{\tau_{Ohm}} \tag{2.24}$$

where B_{res} and $\dot{B}_{res}$ are the field strength in the interior of the core and its rate of change, in contrast to the total core field B_c. We refer to this as the "DELAYED - model': The field evolution of single pulsars according to predictions of the "DELAYED - model" for various assumed values of τ_{Ohm} are shown in Fig. 2.10 , where the results of the original model (referred to, in the present discussion, as the "INSTANT - model"; cf. Eq. 2.18) are also presented for comparison. The predicted field evolution of solitary pulsars and its dependence on the value of crustal decay time scale τ_{Ohm} is seen to be similar according to both the models used in Fig. 2.10. We thus conclude that possible accumulation of expelled flux at the core-crust boundary does not have any significant effect on the predictions of SIF for ***solitary pulsars.*** Note however the interesting feature in Fig. 2.10 that longer values of τ_{Ohm} tend to produce smaller surface fields in old solitary stars. The feature being the same in both the original SIF model (ie. (the

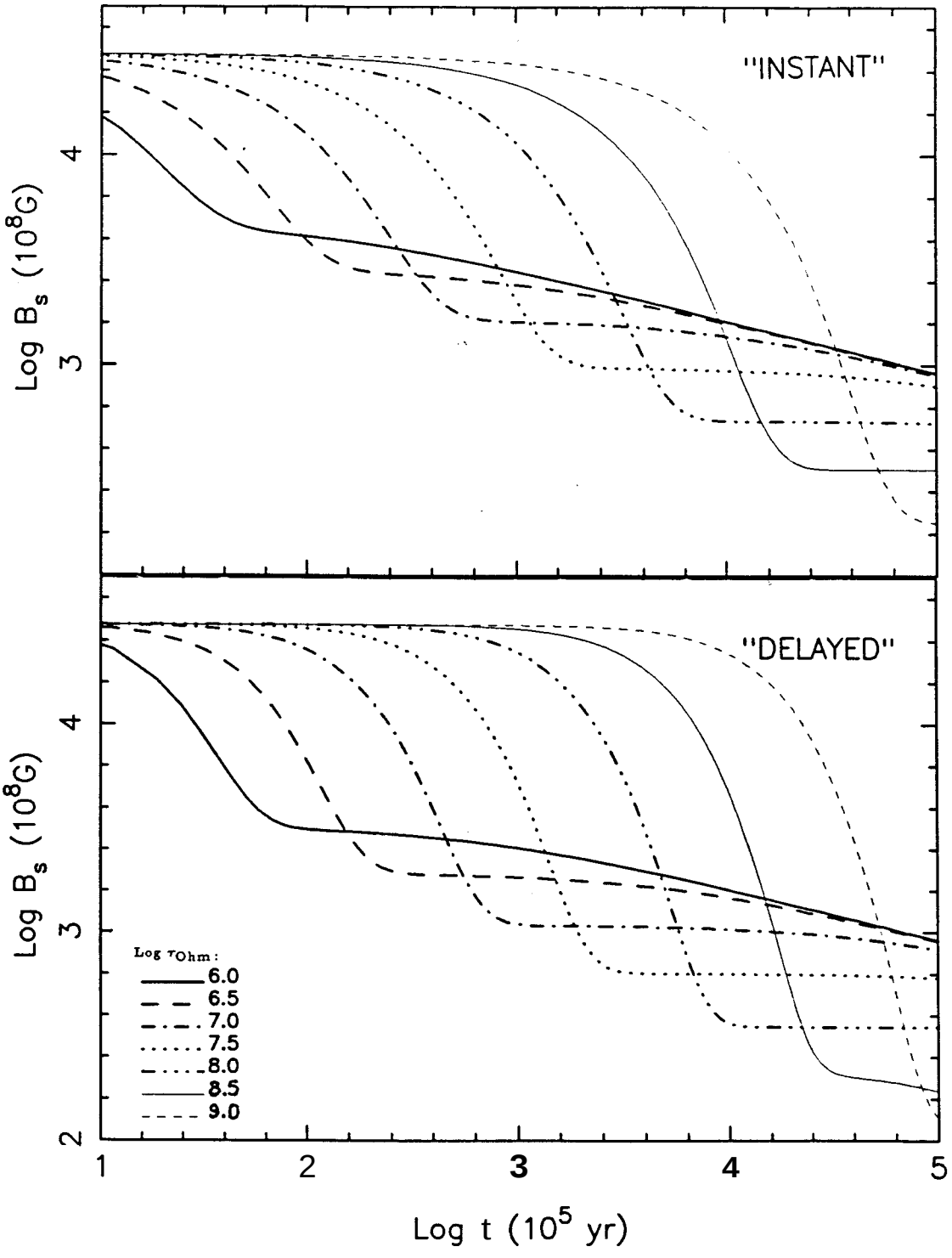

Figure 2.10- Magnetic field evolution of solitary pulsars are shown for the different values of the decay time scale in the crust τ_{Ohm} indicated in units of years, according to predictions of the two versions of the flux expulsion scenario marked as "DELAYED" and "INSTANT" separately.

"INSTANT" model in Fig. 2.10) and the "DELAYED" model explored here.

For evolution of neutron stars in binary systems, the delayed release of the expelled flux causes the surface field to remain stronger for a greater length of time, and hence the neutron star can attain a longer spin period. This results in the eventual expulsion of somewhat larger amount of flux from the interior. Given enough time, the final surface field strengths thus fall below those obtained in our earlier models. The effect is expected to be most pronounced in binaries with longer periods. The predicted final surface fields according to the "DELAYED" model for neutron stars evolved in low-mass binaries are shown in Fig. 2.11 against the initial orbital periods, which show a good agreement with the observational data indicated by the ***circles*** (cf. Table 2.1). Comparison between Fig. 2.11 and Fig. 2.8 indicate that while for the longer period systems ($P_{\rm orb} \sim 100$ day) the neutron star is spun up to longer periods and hence the final surface fields are lower in the "DELAYED" case (for the same values of parameters), but models with shorter periods are hardly affected. Therefore, to reproduce the observed trend of surface magnetic field versus orbital period one needs in this scenario smaller Ohmic time scales in the crust. Our calculations show that with $\tau_{\rm Ohm} \sim 10^8$ yr one can obtain a correspondence with observations of nearly the same degree as in Fig. 2.8.

It might also happen that the building up of fluxoid layer just below the crust reacts on the motion of fluxoids from the interior; perhaps reducing the effectiveness of pinning interaction between neutron vortices and proton fluxoids. However, no quantitative estimate of this is available at this point in the literature to enable us to incorporate it into our models. If this effect is severe it might not be possible in this scenario to achieve a reduction in the surface magnetic field to values comparable to those of the millisecond pulsars.

Spin Periods in LMXBs:

A further observational constraint on the coupled spin-magnetic evolution of neutron stars in low-mass systems is provided by the observed spin periods in LMXBs. In

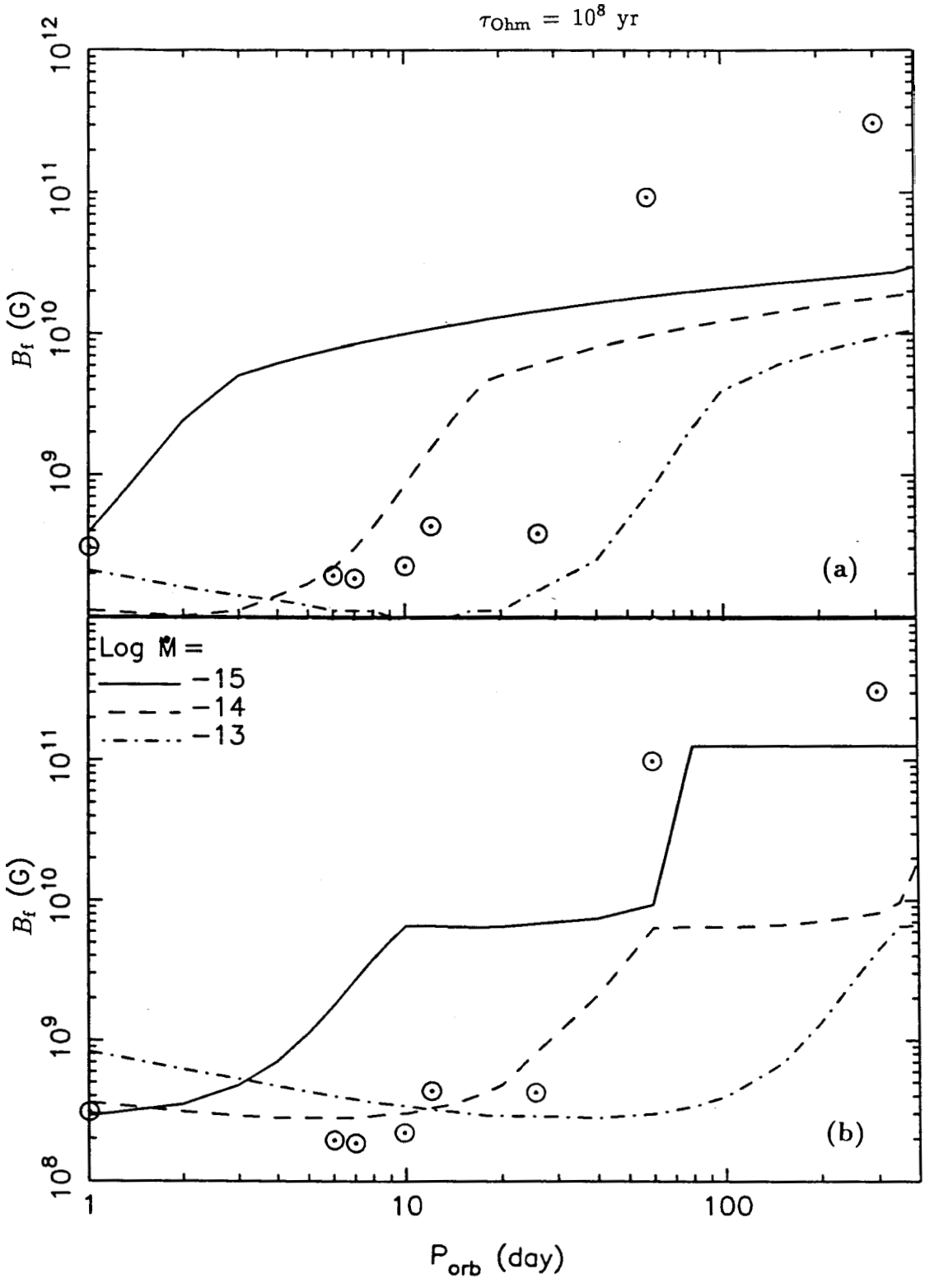

Figure 2.11- Same as Fig. 2.8a, but for the case of the delayed expulsion of the flux out of the core. Initial values of $B_c = B_s = 3$ x 10^{12} G.; and **(a)** initial $P_s = 0.1$ s, $\xi = 0.2$ and (b)initial $P_s = 0.4$ s, and $\xi = 1.0$ have been used.

Fig. 2.12 the predicted distribution of P_x vs P_{orb} in these systems based on SIF, and also the exponential decay model, are shown separately. The values of P_x (spin periods at the *beginning* of the X-ray phase in LMXBs) as predicted in the exponential model are seen to be very small ($\lesssim 10$ s) for values of the Ohmic decay time scale $\tau_{Ohm} \lesssim 10^8$ yr. Larger values of $P_x \gtrsim 100$ s could be reproduced in the exponential scenario only with an assumed large value of $\tau_{Ohm} \gtrsim 10^{8.5}$ yr. Although there is not much observational data available on the spin periods in LMXBs, a value as large as 114 s has been already observed for G X 1+4 (Nagase 1989). Such an observed value for the *present* spin period in an LMXB source implies that the upper limit for the actual values of P_x is much larger than ~ 100 s; values which are difficult to accommodate in the exponential model with any reasonable value of τ_{Ohm}. The SIF model does, however, predict such large values of P_x for various choices of the value of the decay time scale in the range $10^7 \lesssim \tau_{Ohm}(yr) \lesssim 10^9$, as shown in Fig. 2.12.

2.4.3 Globular Cluster Pulsars:

The distribution of the observed radio pulsars in the B, $-$ P, plane (Fig. 2.1) shows that no observed disk-population pulsar lies in the region with $10^9 \lesssim B_s \lesssim 10^{10}$ G. As will be discussed later in § 2.4.3 there is no consensus whether this is a genuine forbidden "gap" for the recycled pulsars or is due to some observational selection effects. This suspected "gap" in the B, $-P_s$ plane which does not accommodate any disk-population observed pulsar is *not* however devoid of pulsars recycled in globular clusters as is seen in Fig. 2.13. The difference can be traced, in the context of the SIF scenario, to the different formation mechanisms which are generally assumed for the progenitor low-mass binaries in the two environments. While for the disk-population systems the neutron star is believed to be born in the binary itself, in the case of globular clusters the binary formation is explained mainly as a result of exchange and/or capture processes. At the time of capture and formation of a binary the neutron star is therefore expected to be an old dead pulsar (with an age $>$ few x 10^9 yr) and have a surface field strength ~ 2 orders of magnitudes smaller than at birth (cf. Fig. 2.6a). The spin and magnetic

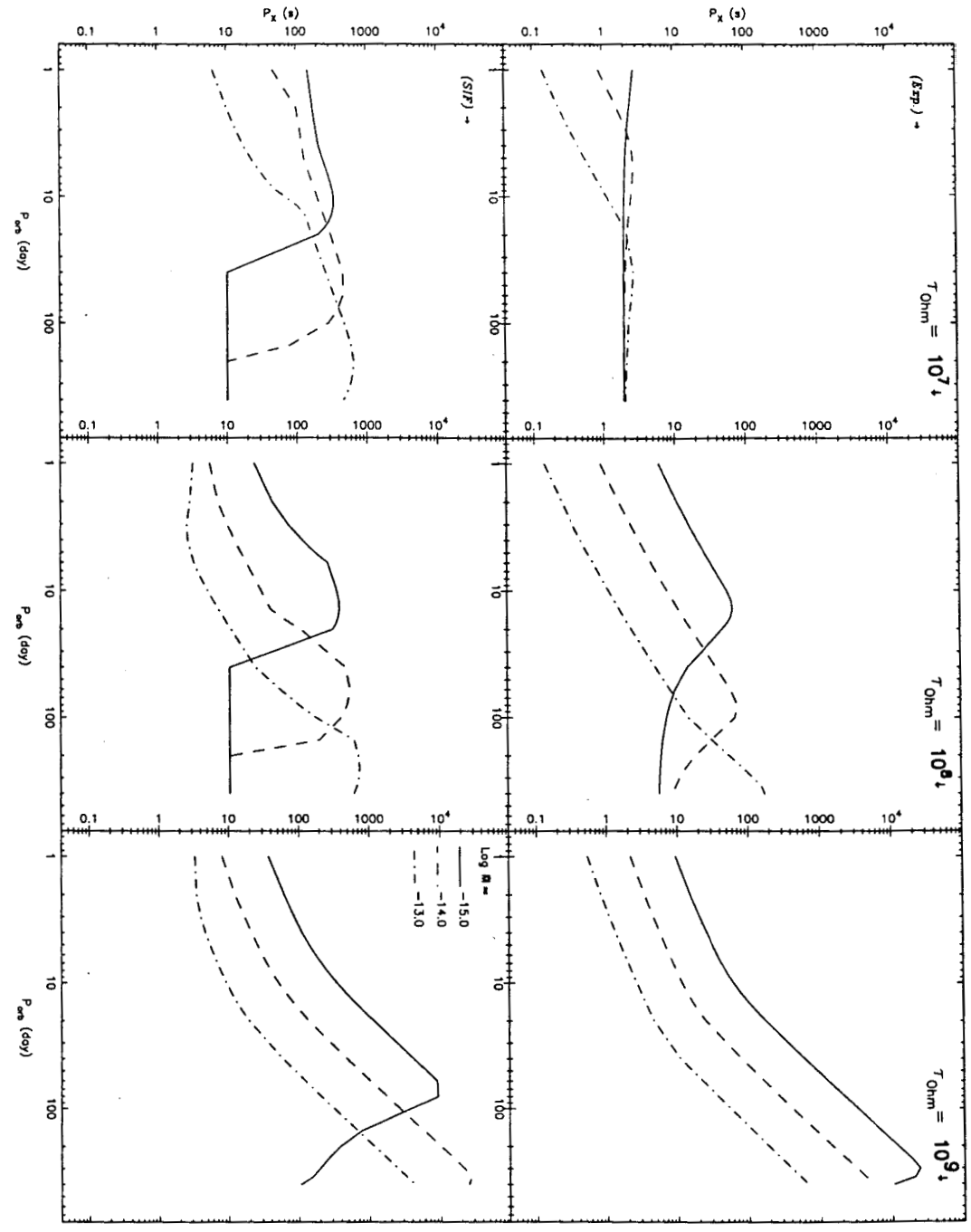

Figure 2.12- Spin periods of neutron stars at the beginning of the LMXB-phase versus orbital periods as predicted in the spin-down-induced flux expulsion scenario scenario (the bottom row marked *SIF*) and in the pure exponential field decay model (the top row marked ***Exp.)***. Each two panels in the same column are for an assumed value of $\tau_{\rm Ohm}$ as indicated (in units of yr). Each curve corresponds to a value of mass-loss rate $\dot{M}_2$ (in units of $M_\odot/\,{\rm yr}$) for the companion star.

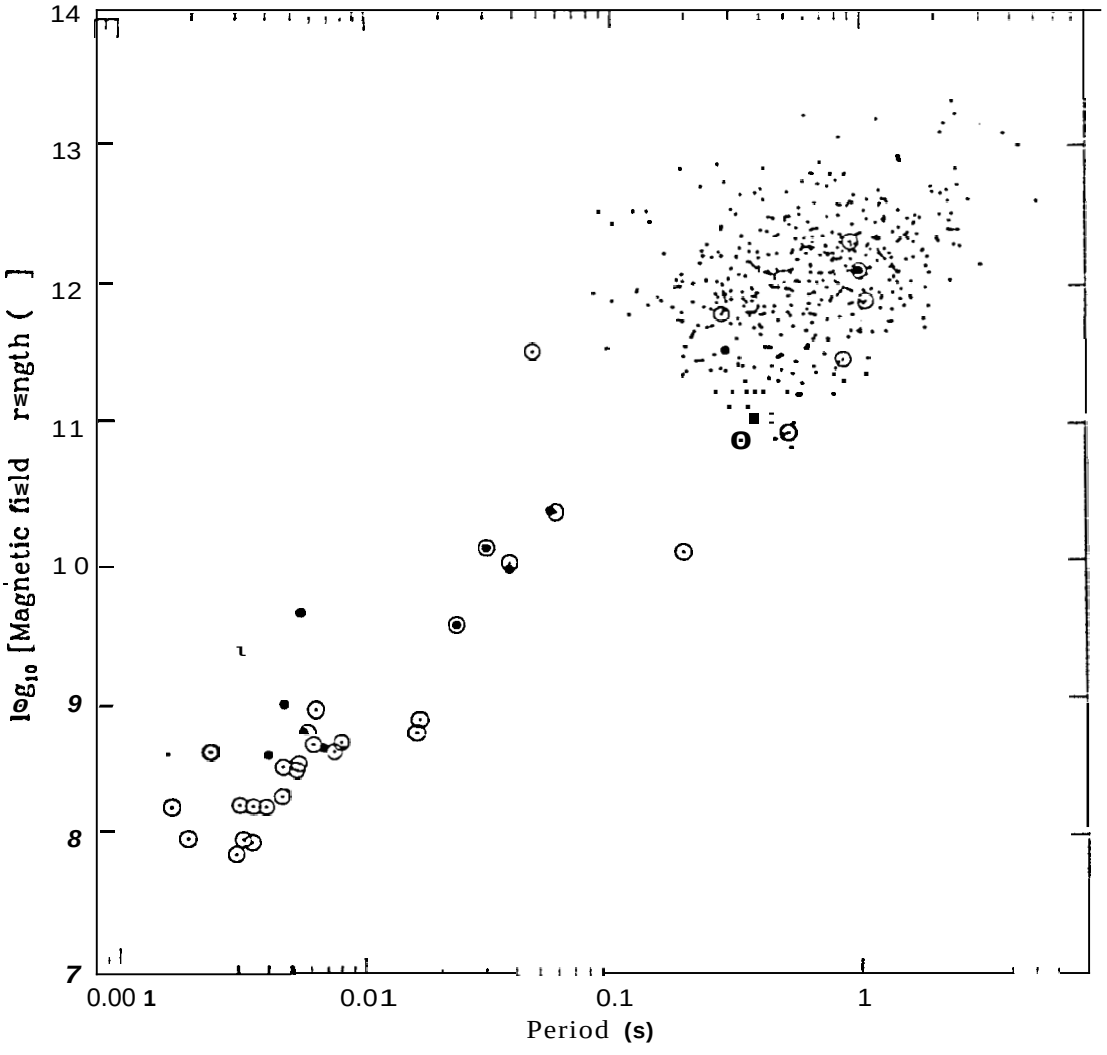

Figure 2.13- Distribution of the measured spin periods P_s and inferred surface magnetic fields B_s of the observed radio pulsars. Single pulsars are shown by small *dots* while presence of a binary is denoted by a surrounding *open circle.* Pulsars thought to be associated with the globular clusters are shown by *filled circles.* Most of the globular cluster pulsars lie in the so-called "gap" region which is almost free from *disk* pulsars (compare with Fig. 2.1). Three of the globular cluster pulsars lie however in the region occupied by the majority of normal Galactic pulsars (the pulsar "island"). [adopted from Lyne, Manchester, & D'Amico 1996]

evolution of such a neutron star in a binary with a low-mass star will be however different from that of a young pulsar with a much stronger field. This is because a lower field strength implies a smaller-size magnetosphere during the spin-down interaction phase and hence the conditions for a spin-up phase would be reached at a smaller value of P_{max} corresponding to a larger value of B_f.

Fig. 2.14a shows the computed values of B_f versus P_{orb} for the two extreme sets of the initial conditions expected for the neutron stars processed in low-mass binaries in globular clusters. Initial values (at the onset of binary evolution) of the magnetic fields and spin periods appropriate for the old neutron stars at the time of binary formation in globular clusters are assumed to be $10^{10.5} \lesssim B_i$ (G) $\lesssim 10^{11}$ and $1 \lesssim P_i$ (s) $\lesssim 5$ based on the results of the single pulsar evolution in Fig. 2.6a. For comparison, the results for the assumed initial values of $B_i = 10^{12.5}$ G and $P_i = 0.1$ s are also shown as a typical case of the disk-population systems. The final field strengths for the globular cluster systems are predicted to have values in the range $10^9 \lesssim B_f$ (G) $\lesssim 2 \times 10^{10}$ as indicated by the two curves in Fig. 2.14a corresponding to the limiting values of the assumed range of initial conditions. The observed values of surface fields of the recycled pulsars in globular clusters which fall in the range $10^{8.5} \lesssim B_s$ (G) $\lesssim 10^{10.5}$ would thus represent their final residual field strengths corresponding to the values of P_{max} which they had attained earlier, and no further decay during their subsequent evolution would be expected.

As already discussed in § 2.4.2 values of $\xi \gtrsim 10$ are needed in order to get good fit with the data on recycled pulsars with low-mass companions (LMBPs) if values of $\tau_{Ohm} < 10^8$ yr are used in our simulations. We have used values of $\tau_{Ohm} = 10^7$ yr and $\xi = 100$ in Fig. 2.14a in accord with the our results far solitary pulsars (see § 2.3) and recycled in massive binary systems (to be discussed in § 2.4.4) which was also justified for the case of recycling in low-mass binary systems (see Fig. 2.9). Nevertheless, as is shown in Fig. 2.14b the larger final field strengths predicted for the initial conditions appropriate to globular clusters holds valid for either combination of values τ_{Ohm} and ξ suggested in § 2.3, namely $\tau_{Ohm} > 10^8$yr and $\xi \lesssim 1$ or $\tau_{Ohm} \sim 10^7$yr and $\xi > 10$.

Following our earlier comments in this chapter about the model of accretion-induced

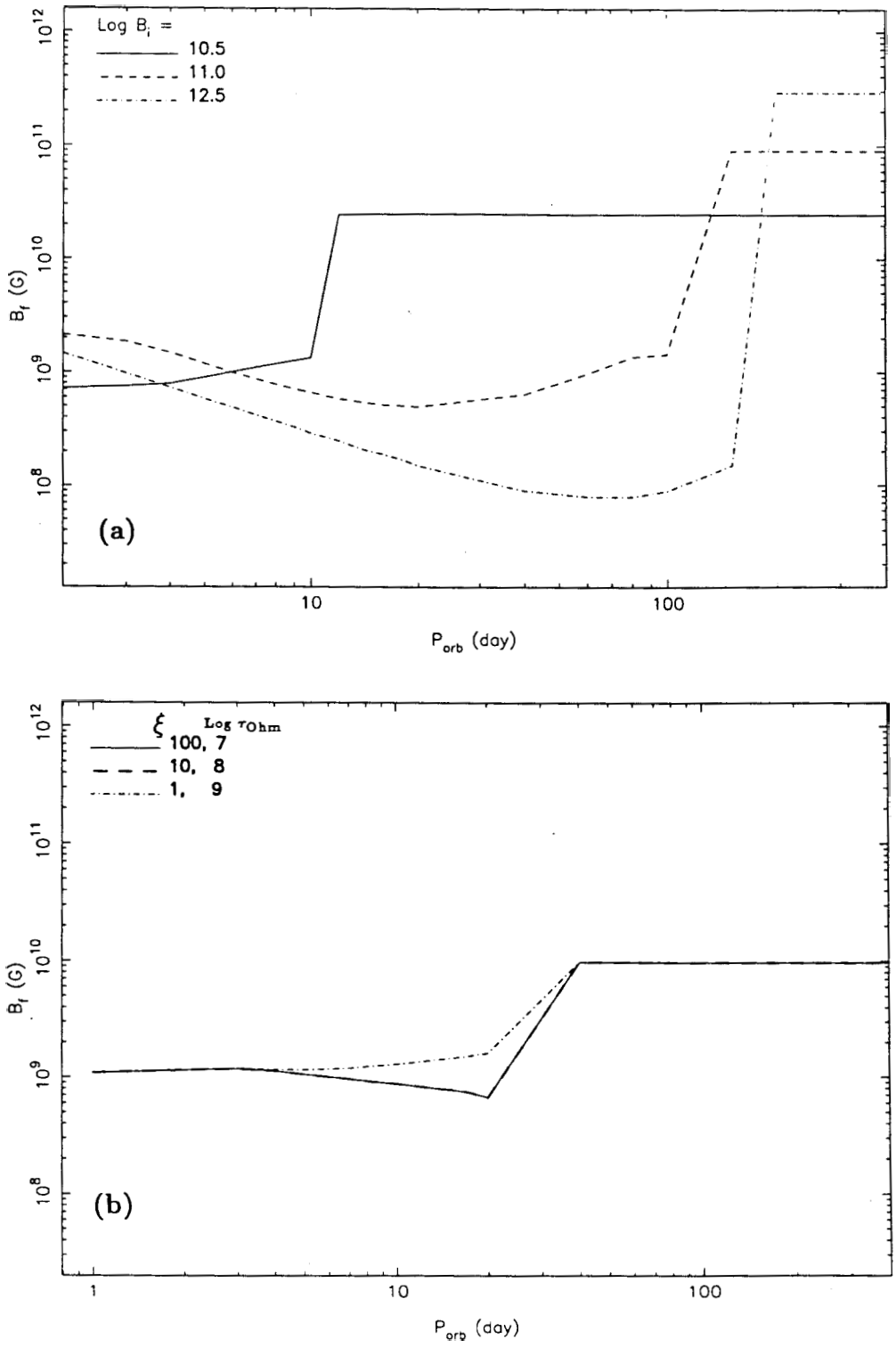

Figure 2.14- a) Final values of the surface magnetic field strengths of neutron stars evolved in low-mass binaries with various orbital periods and for the different assumed initial magnetic field strengths which are appropriate to the globular cluster (the full and the *dashed* lines). Also a case corresponding to the disk population systems is indicated (the *dash-dotted* line). Values of $\dot{M}_2 = 10^{-14}\ M_\odot/yr$, $\xi = 100$, and $\tau_{Ohm} = 10^7$ yr have been assumed. **b)** Same as (a) but for a single value of the initial field strength and for the different combinations of values of τ_{Ohm} and ξ denoted by the different curves. The corresponding values of ξ and $\log \tau_{Ohm}$ (yr) are indicated for each line. Note that the *dashed line* coincides with the *full line* at all orbital periods.

field decay in neutron stars, we note that the observed distinction between field strengths of recycled pulsars in globular clusters and those of the disk population provides further evidence against this model. As discussed above the expected difference between the spin histories of neutron stars in the two types of environments can successfully account for the difference in the final field values according to the SIF model. However there is no reason to expect that the final Roche-lobe accretion phase and hence the predicted fields according to the accretion-induced model should be different.

2.4.4 Massive Progenitors

In this section we discuss the predictions of the SIF model of field decay in neutron stars for those processed in binary systems with massive companion stars, in contrast to the 1 $M_{\odot}$companion which was investigated in § 2.4.2. The coupled spin-magnetic evolution of neutron stars in binary systems with different assumed intermediated- (IM) and high-mass (HM) companion stars was followed throughout the mainsequence lifetime of the companion star. The values of parameters adopted for the companion stars in our models are listed in Table 2.2.

Table 2.2- Values of parameters for the assumed companion stars

companion star	mass ($M_{\odot}$)	lifetime (yr)	mass-loss rate ($M_{\odot}\mathrm{yr}^{-1}$)	wind velocity ($\mathrm{km\ s}^{-1}$)
IM	4	2×10^8	$10^{-11} - 10^{-9}$	500
HM	9	3×10^7	$10^{-10} - 10^{-8}$	600
HM	15	1.2×10^7	$10^{-10} - 10^{-6}$	700
Be-type	9	3×10^7	$10^{-10} - 10^{-8}$	200

The predicted evolution for the spin period, and core and surface fields are shown in Fig. 2.15 which show a characteristic behavior similar to that in the case of low-mass systems in Fig. 2.7a. As there are not many readily identifyable recycled pulsars and further since the true ages of those known are uncertain we are not able to compare

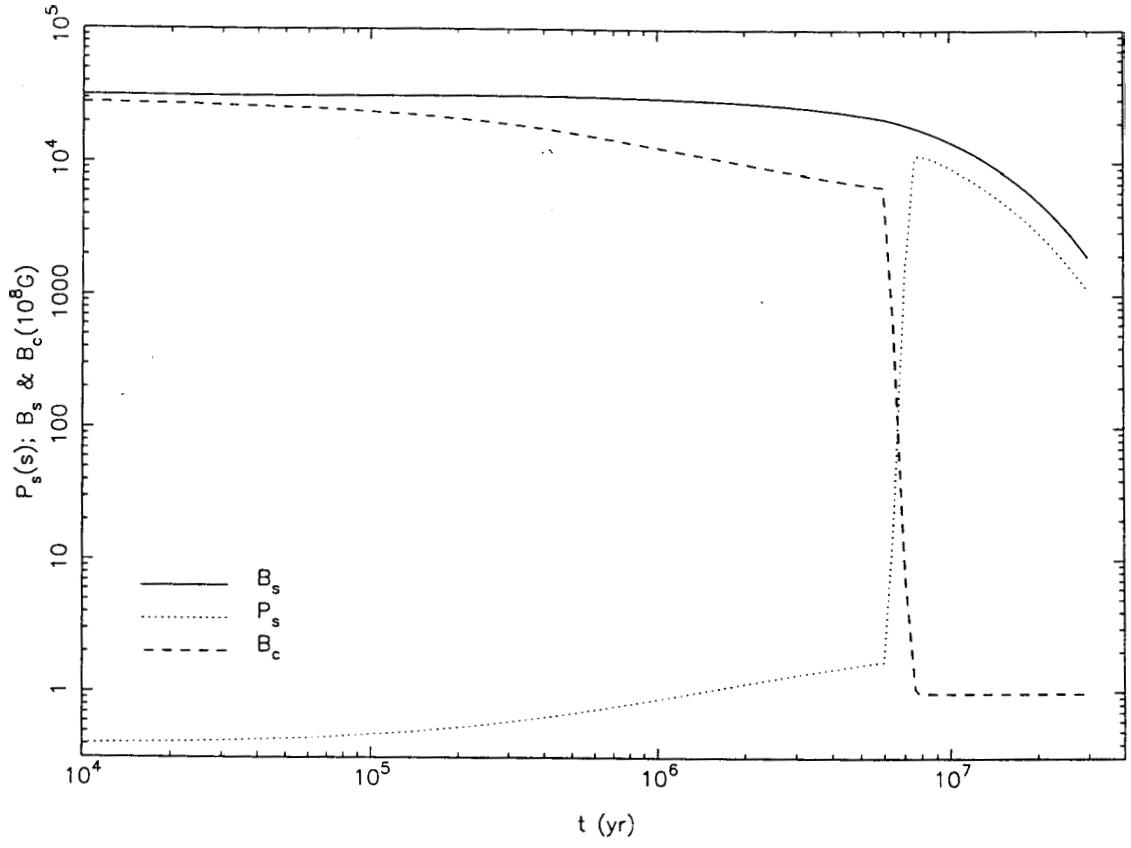

Figure 2.15- Evolution of the spin period P_s, and the magnetic field strength in the core B_c and at the surface B_s of a neutron star in a binary with a massive mainsequence companion, according to the spin-down-induced **flux** expulsion scenario. Values of companion mass $M_2 = 9\ M_\odot$, wind rate of the companion star $M_2 = 10^{-9}\ M_\odot/\mathrm{yr}$, wind velocity $V_w = 600$ km/s, and Ohmic decay time scale $\tau_{Ohm} = 10^7$ yr have been used.

the predicted field evolution with observational data as we did for the case of low-mass systems in Fig. 2.8 and Fig. 2.9. In contrast, identification of the pulsars recycled in the low-mass systems is generally agreed upon, and their present characteristic ages set a minimum limit on the age of the system. Instead we will use the predicted spin evolution (which is according to SIF coupled and influenced by the field evolution) in comparison with the corresponding observed systems to gain some confidence on the results of our simulations. Based on the derived values for the maximum spin periods achieved in these binary systems the expected field evolution of recycled pulsars are then discussed and contrasted with the existing observational constraints.

The predicted final spin periods are plotted against orbital periods in Figs 2.16a & b for systems corresponding to the "standard" and "Be-type" massive X-ray binaries (HMXBs), respectively. The sharp drop and the following flat portion in the predicted periods at large orbital periods is due to the fact that the *propeller phase is never realized in the binary*. The pressure of the pulsar wind overcomes the gas pressure and the pulsar spins down due only to its radiation reaction torque. The observed spin and orbital periods in HMXBs (Waters & van Kerkwijk 1989) are also indicated in each case which show a distribution consistent with the computed curves for the case of $\tau_{\rm Ohm} = 10^7$ yr. In addition to the uncertainties due to the exact values of the mass-loss rates the following points has to be also noted while inspecting the results in Fig. 2.16. The observed "standard" HMXBs are believed (see eg. Bhattacharya & van den Heuvel 1991) to represent evolutionary stages *later* than the epoch represented by the computed curves which correspond to the *end* of the companion mainsequence phase. Therefore, in an observed standard-type HMXB the larger mass loss rate expected for the companion star during its supergiant phase would have already resulted (particularly for the disk-fed systems indicated by *pluses* in Fig. 2.16a) in a decrease in the spin period as compared to its corresponding calculated P_x value shown in Fig. 2.16a. In contrast, the observed Be-type HMXBs are associated with evolutionary stages *earlier* than the epoch represented by the computed curves in Fig. 2.16. Further decrease in the observed spin period for a Be-type source might therefore occur due to

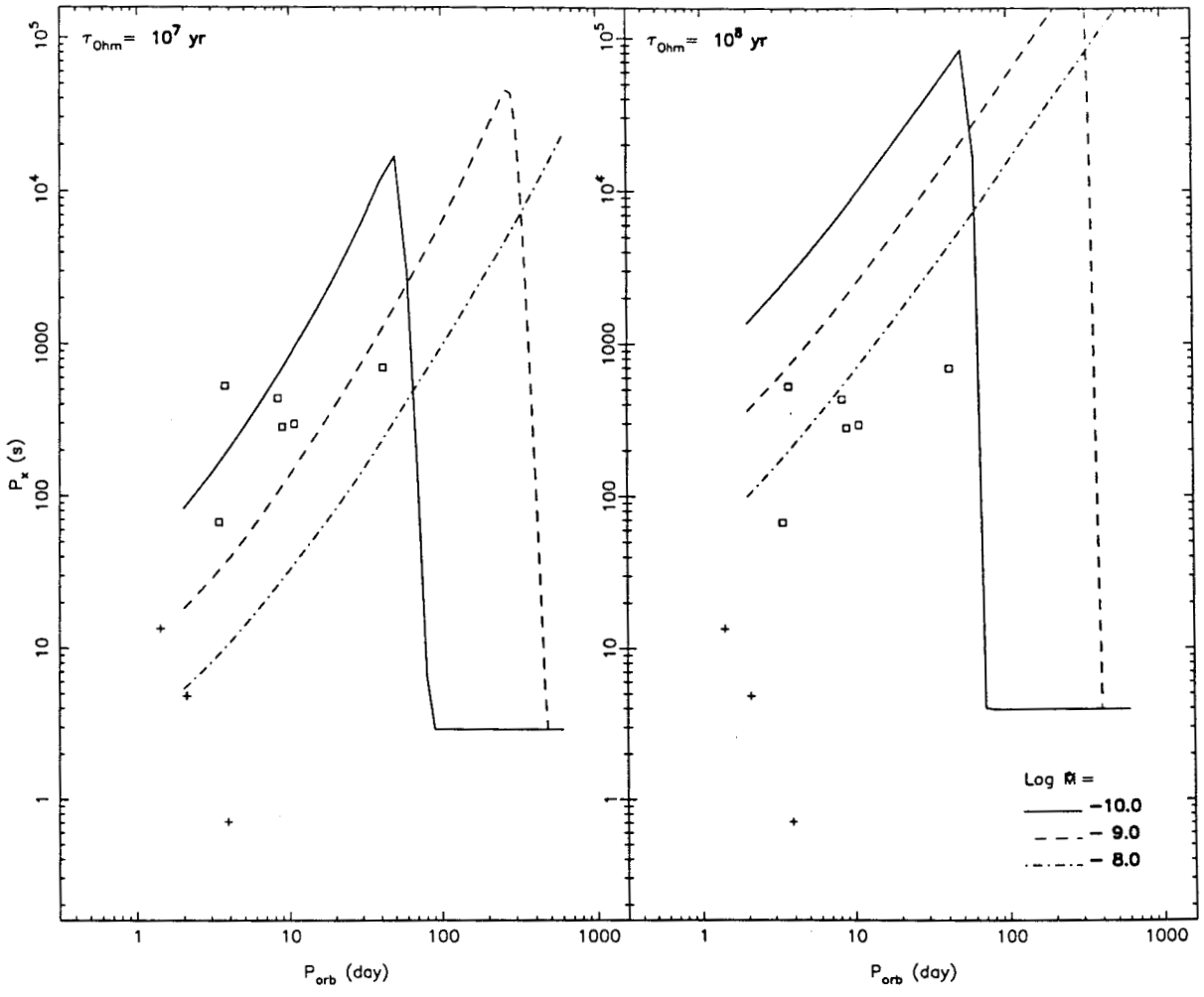

Figure 2.16(a)- Final spin periods of neutron stars processed in binary systems with a 5 $M_\odot$ main-sequence star at the end of its lifetime are plotted against the orbital periods. The two plots are for the two different values of decay time scale, τ_{Ohm}, in the crust as indicated. Each curve corresponds to a different value of mass-loss rate $\dot{M}_2$ (in units of $M_\odot$/ yr) for the companion star. The observed wind-fed and disk-fed "standard" HMXBs (Waters & van Kerkwijk 1989) are denoted by *squares* and *pluses*, respectively.

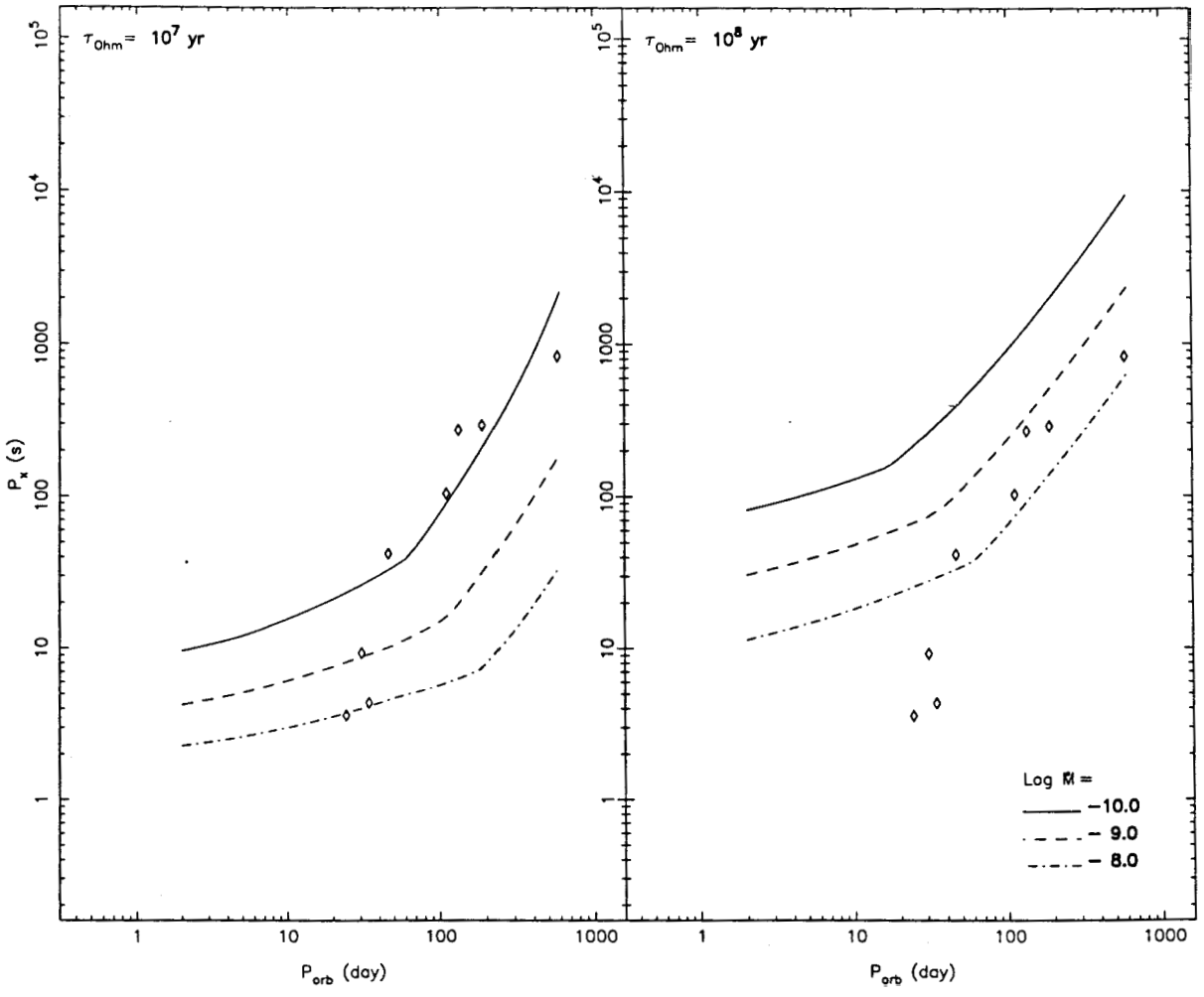

Figure 2.16(b)- Same as Fig. 2.16a, but for a 9 $M_{\odot}$ Be-type companion star. The observed Be-type HMXBs (Waters & van Kerkwijk 1989) are denoted by ***diamonds*** .

a decrease in the field strength before the end of the companion mainsequence lifetime (cf. Fig. 2.16b).

The results of these model computations also indicate that neutron stars evolved in massive close binary systems are generally spun down to large spin periods with values of $\frac{P_{max}}{P_i} \sim 10^4 - 10^5$, for a given value of $P_i \sim 0.1$ s. This implies, as required in the SIF mechanism, an eventual reduction in the magnetic fields of pulsars recycled in close binaries by $4 - 5$ orders of magnitudes, after a long enough time for the crustal field to decay. Even larger values of P_{max} are also predicted for some of the binary systems considered which would result in smaller values of $B_f \sim 10^6$ G. The generally accepted minimum value of $B_f \sim 10^8$ G for the residual fields which might be true for pulsars recycled in binaries with low-mass companions, and in good agreement with predictions of the SIF scenario for these systems (cf. § 2.4.2), seems therefore to be a selection effect imposed by the pulsar "death"-line (§ 2.4.2) on the observable spin periods and magnetic fields. We note that while our results for the large values of P_{max} are based on an assumed "propeller" spin-down mechanism other processes responsible for a spinning down of an accreting neutron star have also been proposed which are expected to be effective in cases where the "propeller" mechanism fails or is argued not to be very efficient (Mineshige, Rees & Fabian 1991; Illarionov & Kompaneets 1990). Also, while a value of $\xi = 1$ has been used in Fig. 2.16 larger values of ξ which were necessary in the case of low-mass systems for assumed values of $\tau_{Ohm} \sim 10^7$ yr do not however have much effect on our results for the values of P_{max} (hence B_f) in the case of binaries with massive companion stars.

Our following discussion of the predicted field evolution of pulsars recycled in massive systems will be divided into two parts corresponding to systems with intermediate- or high-mass companion stars for the neutron star. Recycled binary pulsars from these systems will have massive C-O white dwarf or neutron star companions, respectively, and will be referred to as IMBPs and HMBPs (if the binary survives after the birth of the second born neutron star). The adopted masses and lifetimes for the intermediate- and high-mass stars, based on the stellar evolution results of Schaller et al. (1992)

for solar metallicities, are given in Table 2.3. We note however that longer lifetimes for massive stars which are predicted due to a different treatment of the convection problem and the opacity in the stars (eg. Bressan et al. 1993) would imply a somewhat larger upper limit on the acceptable values of $\tau_{\rm Ohm}$ inferred from the following considerations.

Table **2.3-** Classification of the massive stars

star	mass ($M_\odot$)	lifetime (yr)
IM	$2.5 - 7$	$7 \times 10^8 - 5 \times 10^7$
HM	$\gtrsim 9$	$\lesssim 3 \times 10^7$

Recycled Pulsars from Massive Binaries:

There are at present two observed binary pulsars with massive compact companions (neutron stars) which have magnetic fields $\gtrsim 10^{11.5}$ G. One of them has a period smaller and the other larger than the corresponding $P_{\rm eq}$ values. These might well be the second born neutron stars in the binary systems and thus part of the population of normal pulsars. Similarly pulsars with $B_{\rm s}$ and $P_{\rm s}$ values consistent with those of normal solitary pulsars but with a white dwarf (WD) companion are not, in general, required to be recycled. **A** late (case B or C, as it is called) mass-transfer to a white-dwarf from its evolved (He or carbon core-burning, respectively) IM companion could result in formation of a pulsar via accretion-induced collapse of the WD. Further evolution of the companion to a WD might be however so rapid that the neutron star could not be spun up to the required value of $P_{\rm eq}$. Binary evolution calculations have shown that a neutron star may in fact be born in a binary even ***after*** the birth of its white dwarf companion (Dewey & Cordes 1987; Pols et al. 1991).

However, recycling in a binary with a very massive and hence short lifetime ($t_{\rm c} \lesssim \tau_{\rm Ohm}$) companion could also account for such high field pulsars with periods larger than $P_{\rm eq}$ which might be ***single*** or in double neutron star binaries. This possibility which is indicated by ***track 1*** in Fig. 2.17 had been already considered as the cause of a detected

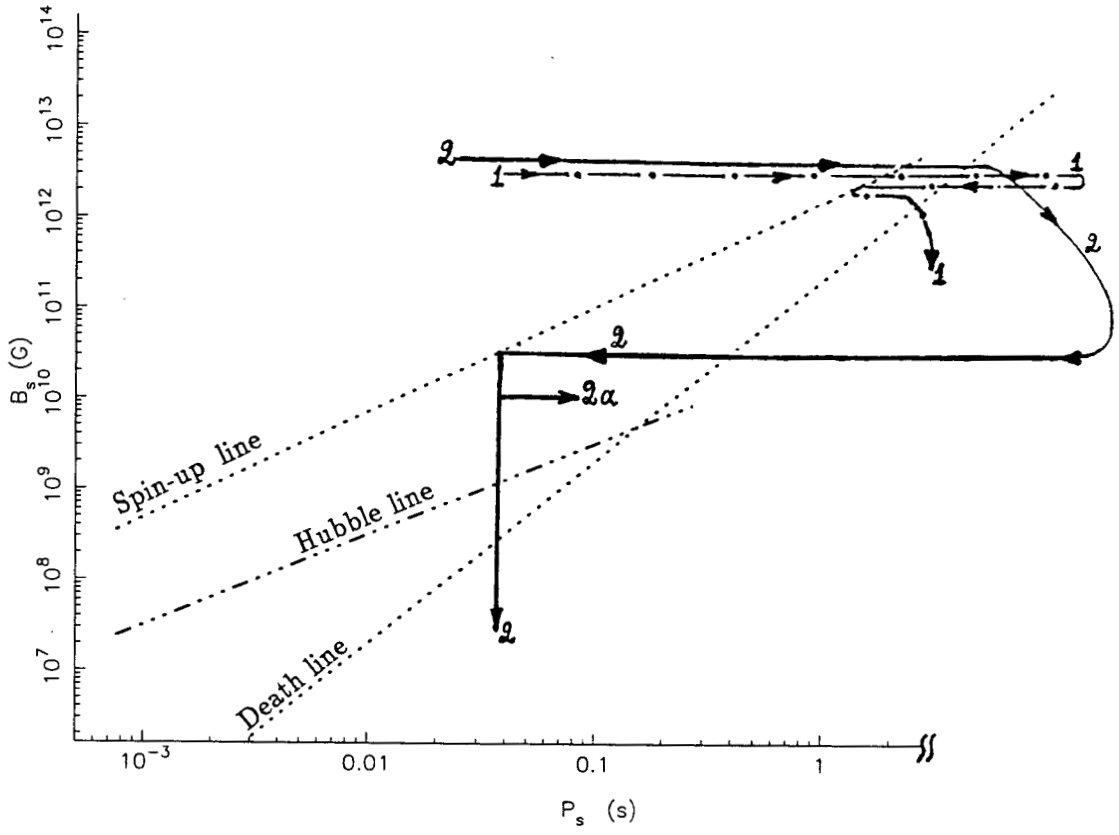

Figure 2.17- Schematic representation of the predicted recycling routes for evolution of the magnetic fields and spin periods of neutron stars in binary systems with ***high-mass*** companion stars according to the spin-down-induced flux expulsion scenario.

increase (an "injection") in the "current" of pulsars (Deshpande, Ramachandran, & Srinivasan 1995). The "current" of pulsars on the $B_s - P_s$ plane, due to the spin-down of the star, from a bin of width ΔP_s at given values of P_s and B_s is defined as $J(B_s, P_s) = \frac{1}{\Delta P_s} \sum_i P_{si}$, where the sum extends over all pulsars in the Galaxy that fall into the bin. The prominent '(injection" effect has been detected at the large field values (Deshpande, Ramachandran, & Srinivasan 1995) as shown by *track 1* in Fig. 2.17.

On the other hand, pulsars like **PSR** B1913+16, **PSR** B1534+12, and any other binary or single pulsar with similar periods (P, $\sim$ 0.06 s) and $B_s \lesssim 10^{10.5}$ *G* imply a recycling history in a binary with a companion having a lifetime $t_c \sim (3 - 6)$ times the value of the decay time scale of the crust τ_{Ohm}. The post-recycling evolution of such pulsars would be in general first along vertical tracks *(track 2* in Fig. 2.17) on the $B_s - P_s$ plane while the field decays on a time scale $\sim \tau_{Ohm}$ down to its final value (Eq. 2.9) and is then followed by a horizontal path *(track 2a* in Fig. 2.17). **A** value of $P_{eq} \sim 0.01$ **s** corresponding to $B_R \sim 10^{10}$ G is predicted (Eq. 2.8) to be the lowest possible value achieved in binaries with HM-companions for an assumed value of $\tau_{Ohm} \sim (1-2)$ **x** 10^7 yr (preferred by the results in Fig. 2.16) and the adopted range of lifetimes for HM-stars: Larger values of τ_{Ohm} would imply larger B_R values which would not readily account for the observed systems.

However, lower values of B_R, and hence P_{eq}, might also be entertained for these systems if one allows for the possibility of a *temporary reduction in the Ohmic decay time scale* of the crustal field. One way to achieve this is through a temporary compression of a large amount of magnetic **flux** into a narrow region at the bottom of the crust. Such an enhanced field compression might be expected to occur in the context of the SIF scenario only for the case of massive binaries in which the short spin-down time scales could result in **flux** expulsion out of the core at a rate faster than its assumed rate of diffusion into the upper regions of the crust. Compression of the current-carrying layers of the crust with the effect of a reduction in the length scale of the field distribution has been considered to occur also as a result of the matter accreted onto the neutron star (Konar, Bhattacharya & Urpin 1995). The accretion-induced field decay

for the crustal fields of neutron stars is not however expected to have any significant effect for the predictions of SIF in the case of long-lived low-mass systems. This is because accretion of a substantial amount of matter in these systems occurs, namely during the Roche-lobe overflow phase, only after the crustal fields have already decayed down to very negligible values. Short decay time scales ($\sim 5 \times 10^6$ yr) associated with a compressed flux in the high-density region at the bottom of the crust have also been suggested based on the effect of a magnetic buoyancy force. A Hall drift is expected to occur due to the buoyancy force with a radial component that would deposit the flux into the outer regions of the crust where it is subject to a more rapid Ohmic diffusion (Jones 1988).

The above possibility of a temporary increase in the rate of field decay in the crust also might resolve the disagreement between field strengths among X-ray pulsars and the recycled pulsars which are born from them (cf. § 2.1.1). The apparent inconsistency between the inferred surface fields of neutron stars in HMXBs and those in the double neutron star binaries might be alternatively resolved by assuming a low-field population of HMXBs that are not however expected to be observable as X-ray pulsars, as mentioned earlier (cf. § 2.1.1). These two possibilities for the magnetic history of a recycled pulsar similar to PSR B1913+16 namely a short-term enhanced filed decay or a low-field HMXB progenitor are invoked in the different evolutionary routes considered for the recycled pulsars in Tables 2.4 and 2.5.

Pulsars from Intermediate-Mass Binaries:

Neutron stars recycled in binaries with intermediate-mass companion stars (IMBPs) are predicted (cf. Eq. 2.8), for the assumed values of $\tau_{\rm Ohm}$ and lifetimes of the companion star, to achieve values of $P_{\rm eq}$ corresponding to $10^9 < B_{\rm R} < 10^{10}$ G, namely in the region which is sometimes referred to as the "gap" in the $B_s - P_s$ plane (eg. Kulkarni 1995). The subsequent evolution of these pulsars would be decided (cf. Eq. 2.9) by the value of $P_{\rm max}$ that they had attained earlier which in turn depends on the properties of their progenitor binary systems. The results of our model computations for the case of a

4 $M_{\odot}$ companion star show that binaries with smaller orbital periods (in the range of interest for a case-B Roche-lobe overflow mass transfer which is believed to occur in these systems) and/or larger stellar wind rates would give rise to smaller values for $P_{\rm max}$.

Pulsars recycled in such binaries would consequently live with no further substantial decay in their magnetic fields after recycling, given a low enough mass for the companion star and hence a long enough time for their initial fields to decay. This possibility is indicated by track *1* in Fig. 2.18. Such an evolutionary history with a value of 30 ms $\lesssim P_{\rm eq} \lesssim$ 190 ms might be assumed for PSR B0655+64. Larger values of $P_{\rm max}$ which are predicted for the wider binaries would imply (given a value of $t_{\rm c} \lesssim 10^8$ yr) a behavior for the recycled pulsar (track **2** in Fig. 2.18) similar to that of the descendants of binaries with high-mass companion stars indicated by track 2 in Fig. 2.17. The final evolution of the pulsar might be as well along a horizontal path (track *2a* in Fig. 2.18) depending on the value of $P_{\rm max}$ it had achieved. PSR J2145-0750 and also possibly PSR J1022+1001 (Camilo et al. 1996) might be considered as examples of the latter type of evolution in IMBPs. A value of 10 ms $\lesssim P_{\rm eq} \lesssim$ 16 ms and a subsequent downward evolution on the $B_{\rm s} - P_{\rm s}$ plane in both cases are consistent with their observed properties as well as the model predictions. Also, the observed larger $P_{\rm orb}$ in the latter two pulsars (as well as the smaller companion mass in the case of PSR J2145-0750) than for PSR B0655+64 are in agreement with the above criteria for occurrence of the two types of post-recycling evolution in IMBPs (to the extent that the initial orbital periods and companion masses of their progenitor systems can be ascertained).

Furthermore, the predicted post-recycling evolution of IMBPs down vertical tracks might also explain the fact that none of the observed (disk-population) pulsars lie in the "gap" region on the $B_{\rm s} - P_{\rm s}$ plane (see Fig. 2.1) although it is generally expected that the region should be occupied by IMBPs. The problem has been recently further highlighted since considerations based on the frequency and survival probability of progenitor binaries of IMBPs as compared to LMBPs has led to the conclusion that the observed number of IMBPs is much less than the expected value (Kulkarni 1995). This

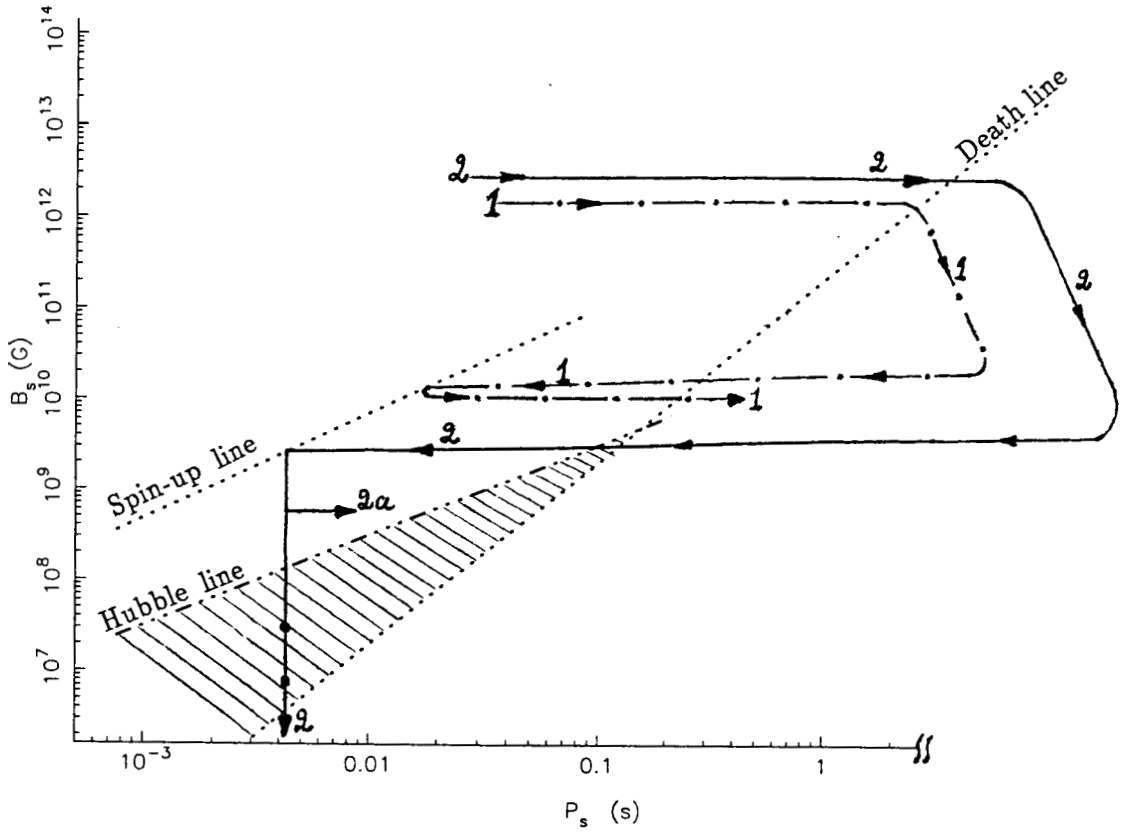

Figure 2.18- Schematic representation of the predicted recycling routes for evolution of the magnetic fields and spin periods of neutron stars in binary systems with *intermediate-mass* companion stars according to the spin-down-induced flux expulsion scenario.

is because recent theoretical considerations of binary-stellar evolution in progenitors of these systems predict that contrary to earlier belief their spin-up Roche-lobe overflow phases are long and efficient enough to spin the accreting neutron stars in these systems up to millisecond periods (Bhattacharya 1996). Possible explanations suggested including the one invoked here for the paucity of IMBPs relate it to:

a) the fact that the corresponding progenitors of such pulsars during the accretion-powered X-ray phase are not observed which might be itself due to

   - an instability in the associated Roche-lobe overflow mass-transfer that would make the duration of the X-ray phase to be extremely short and inefficient (van den Heuvel 1994b) and hence a recycled pulsar would not be born, or
   - that an X-ray phase (hence the spin-up of the neutron star) is not realized at all because of an instability in the first mass-transfer episode in the progenitor binary, namely before the formation of the neutron star due to the large mass ratio of the binary components (Rathnasree 1993).

b) selection effects due to

   - their lower expected radio luminosities in comparison to the millisecond pulsars, and
   - Doppler smearing of the pulsed signal because of the high orbital acceleration of the pulsar being in a tight orbit with a relatively massive companion (Kulkarni 1995).

c) the downward vertical evolution (on a time scale $\sim \tau_{\rm Ohm}$) predicted in SIF for some IMBPs although they are also expected to first appear in the "gap" region. The very large values of $t_{\rm ch} >> \tau_{\rm Ohm}$ at the corresponding $P_{\rm eq}$ and $B_{\rm R}$ where the recycled pulsar starts its new life would however imply that it will spend very little time in the "gap" region.. Furthermore, because of the larger values of $\frac{P_{\rm max}}{P_{\rm i}}$ for IMBPs as compared to LMBPs which is due to the higher stellar

wind rates in IM-stars their fields should decay down to values of $B_f \lesssim 10^7$ G which is smaller than that predicted for LMBPs. Consequently, most of the pulsars recycled in binaries with IM stars are expected to cross the standard pulsar death-line before arriving at their final residual field values.

The suggested downward evolution of recycled pulsars would also allow for the wedge-shape region between the "Hubble"-line ($t_{sd} = 10^{10}$ yr) and the "death"-line to be populated (the *shaded* area in Fig. *2.18).* This is in contrast to the usual assumption that a value of $B_f \sim 10^8$ G is the minimum residual field, and also that recycled pulsars would evolve with essentially no further field decay after recycling. However, the short time scale of the assumed downward vertical evolution of the recycled pulsars in contrast to the much larger values of the characteristic ages in that region would imply a low probability of observing pulsars in this phase of their evolution as was argued earlier for the "gap" region. In addition, the pulsar death-line has been suggested to have a smaller slope in the region of $B_s \lesssim 10^9$ *G* based on additional constraints on the e^+e^- pair creation in the vacuum gap invoked in the polar cap theories of radio emission mechanism of pulsars (Phinney & Kulkarni *1994;* Rudak & Ritter *1994;* see also Chen & Ruderman *1993).* The modification of the death-line will have the effect of reducing the area of the wedge-shape region between the death-line and the Hubble-line and hence reducing the expected number of the recycled pulsars in that region. Nevertheless, at least one pulsar has been already observed which belong to this region, namely PSR J2317+1439 with a $P_f = 3.443$ ms and a $B_f = 10^{7.96}$ *G* (Camilo, Nice & Taylor *1993).* The observed properties of this pulsar can be accounted for in the standard scenario only by assuming a low accretion rate $\dot{M}_{acc} \lesssim 10^{-2} M_{Edd}$ during the Roche-lobe overflow phase of the progenitor LMXB. Similarly the observed recycled pulsars which are believed to be much younger than implied by their characteristic ages (Lorimer et al. 1995b; Camilo, Thorsett & Kulkarni *1994)* might be also accounted for in terms of their rapid downward evolution discussed here.

Summary:

To summarize, a value of $\tau_{Ohm} \sim (1 - 2) \times 10^7$ yr might be suggested for the mean crustal Ohmic decay time scale based on the implications of the SIF scenario for the observed distribution of single and binary pulsars. Given such a value of τ_{Ohm}, pulsars recycled in binaries with high-mass companions are expected to evolve further along vertical tracks on the $B_s - P_s$ plane while those processed in low-mass systems would follow horizontal evolutionary paths. The intermediate-mass companions are predicted to result in recycled pulsars which will have an intermediate behavior between the above two extremes. The results for a larger assumed value of $\tau_{Ohm} \sim 10^8$ yr might be also consistent with the observations as far as the evolution of *binary pulsars* is concerned. Such a value of τ_{Ohm} would however leave the origin of the observed excess in the number of low-field solitary pulsars unexplained. Evolution of HMBPs and IMBPs as discussed here is further summarized in Tables 2.4 and 2.5 where a comparison is also made between the results expected for the two assumed values of $\tau_{Ohm} \sim 10^7$ yr and 10^8 yr.

Four possible evolutionary routes are distinguished in Table 2.4 depending on the values of two observable quantities, namely the strength of the magnetic field in the X-ray phase B_x and its value in recycled pulsars B_f. Route 2 differs from others (1, 3, and 4) in that a large drop in the magnetic filed strength (by a factor of $\gtrsim 10^2$) is assumed to occur *at* the transition from a progenitor HMXB-phase to the descendent recycled pulsar. Routes 3 and 4 in contrast consider the consequences of assuming low-field HMXB progenitors for HMBPs and IMBPs.

Table 2.4- Observationally distinct recycling routes

X-ray source		recycled system	route
pulsating	large B_x $\sim 10^{12}$ G	$B_f \sim 10^{12}$ G	1
		$B_f \lesssim 10^{11}$ G	2
	low B_x $\lesssim 10^{11}$ G		3
non-pulsating			4

The requirements for realization of each route for the two different values of τ_{Ohm} and the expected post-recycling evolution of the neutron star as well as the possible types of its companion star are then shown in Table 2.5. In particular, the possibility of producing recycled pulsars similar to PSR B1913+16 and PSR B0655+64 are also indicated in each case. As can be seen from Table 2.5, while both values of τ_{Ohm} are permitted in the case of an enhanced field decay at the end of the X-ray phase (route 2), however a choice of $\tau_{Ohm} \sim 10^7$ yr has the further merits of being acceptable even without invoking such a rapid field decay besides its success in explaining the origin of the low-field single pulsars.

Table 2.5- The requirements and results of the different recycling routes

assuming				implications for			
route	t_c/τ_{Ohm}	B_R/B_i	τ_{Ohm} (yr)	companion star	post-recycling[e]	1913+16	0655+64
1	$\lesssim 3$		10^8	HM ; IM	horizontal	NO	NO
		$\gtrsim 0.1$	10^7	higher mass HM	vertical	NO	NO
3 &	3 – 10		10^8	lower mass IM	horizontal then vertical	NO	NO
4		$\lesssim 0.1$	10^7	lower mass HM; IM	horizontal then vertical then horizontal	YES	YES
2	temporarily	$> 10^{-4}$	10^7; 10^8	HM ; IM	vertical then horizontal		
	reduced τ_{Ohm}	$\lesssim 10^{-4}$	10^7; 10^8	HM ; IM	horizontal	NO	NO

* horizontal and vertical evolutionary tracks on the $B_s - P_s$ plane.

2.5 Main Conclusions of this Chapter

In this section we gather together all the new results and conclusions arrived at in this chapter. The spin-down-induced flux expulsion model of magnetic field decay in neutron stars leads to the following conclusions :

1. Old solitary neutron stars are expected to have surface dipole field strengths $\sim 10^{11}$ G.

2. The observed populations of single pulsars as a whole can be explained as making a single population born with similar initial conditions. The low-field high-latitude pulsars with no smaller period counterparts could be accounted for by the evolution of some of the larger-field pulsars undergoing a "restricted" field decay that results in an increase (by a factor of $\gtrsim 10$) in their active lifetimes. An "injection" in the "current" of pulsars at larger field values would be due to recycled pulsars in very massive binaries which do not live long enough for the field to decay.

3. Spin periods as large as $P_s \sim 10^3$ s for neutron stars in LMXBs are predicted by the spin-down-induced model of field decay. This should be contrasted with $P_s \lesssim 10$ s to be expected based on the purely exponential field decay model.

4. Magnetic fields of order $10^8 - 10^9$ G observed in millisecond pulsars can be obtained under a variety of circumstances provided either

   - the Ohmic diffusion time scale τ_{Ohm} at the bottom of the crust lies in the range $10^{8.5} - 10^9$ yr, and the spin-down torque due to accreted wind is similar to that of a Keplerian disk interacting with the magnetosphere at a an .interface which corresponds to a value of $\xi = 1$ for the effieciency factor defined for the rate of angular momentum transfer. Or

- a more efficient torque is considered ($\xi > 10$) in which case $\tau_{\rm Ohm} \sim 10^7$ yr would be preferred. This latter choice is preferred as the results for spin-magnetic evolution of solitary pulsars as well as those recycled in massive binaries indicate a value of $\tau_{\rm Ohm} \sim 10^7$ yr.

5. The lowest final surface field strengths B_s achieved for pulsars recycled in low-mass systems in our models are of order 10^8 G. This results from the fact that the maximum spin periods acquired by the neutron stars in the course of their binary evolution never exceed a value of $\sim 10^4$ s, *irrespective of the initial conditions that we have considered.*

6. The broad agreement between the observed trend of final field strengths as a function of the initial orbital period is encouraging, especially in view of the wide range of possible initial conditions that may obtain in wide LMXBs. Extension of the work to the case of very tight orbits ($P_{\rm orb} < 0.5$ day) would provide further constraints.

7. The transport of flux across the core-crust boundary plays a significant role in determining the final surface field strengths of neutron stars. For example, if this transport occurs in a time scale similar to the Ohmic time scale in the crust then the values of $\tau_{\rm Ohm}$ required to explain observations would be an order of magnitude lower than if the above transport is instantaneous. Hence lower values of $\tau_{\rm Ohm}$ would produce acceptable field strengths for low-mass binary pulsars even for small values of the efficiency factor $\xi \gtrsim 1$. More detailed and quantitative models of flux transport in the inner crust would be useful, and probably be necessary, to form a coherent picture of the evolution of the magnetic fields of neutron stars in a wide variety of systems.

8. Recycled pulsars in globular clusters are predicted to have a similar history, and future (!), as those recycled in disk-population low-mass systems *except for their higher residual field values which is a result* of *their lower magnetic fields when they are captured in a binary with their low-mass companions.*

9. Post-recycling evolution of many pulsars processed in binary systems with high- and intermediate-mass companion stars would be along vertical tracks on the $B_s - P_s$ plane, while those with low-mass companions will follow horizontal paths.

10. Recycled pulsars might populate the region between the Hubble-line and the death-line on the $B_s - P_s$ plane, although the rapid downward evolution predicted for such pulsars makes the chance of observing them very small.

11. A value of $B_f \sim 10^8$ G need not be an absolute minimum value for the residual field of neutron stars. Neutron stars recycled in close binaries might attain smaller final magnetic field strengths of $B_f \gtrsim 10^6$ G, although they will be unobservable as radio pulsars unless they are spun-up to sub-millisecond periods.